Modelling of reinvasion efficiency in *Plasmodium falciparum* cultures

by

Maria Magdalena Oosthuizen

Thesis presented in partial fulfilment of the requirements for the degree of Master of Science in Biochemistry in the Faculty of Science at Stellenbosch University

Department of Biochemistry
University of Stellenbosch,
Private Bag X1, Matieland 7602, South Africa.

Supervisor: Prof. J. L. Snoep
Dr. D. D. van Niekerk

March 2017

Declaration

By submitting this thesis electronically, I declare that the entirety of the work contained therein is my own, original work, that I am the sole author thereof (save to the extent explicitly otherwise stated), that reproduction and publication thereof by Stellenbosch University will not infringe any third party rights and that I have not previously in its entirety or in part submitted it for obtaining any qualification.

Date: March 2017

Abstract

Modelling of reinvasion efficiency in *Plasmodium falciparum* cultures

M. M. Oosthuizen

Department of Biochemistry
University of Stellenbosch,
Private Bag X1, Matieland 7602, South Africa.

Thesis: MSc BSc Biochemistry

March 2017

The virulence and severity of the malaria disease within a human host is dependent on how efficient daughter merozoites reinvade red blood cells. Traditionally estimating the efficiency of erythrocytic invasion of *P.falciparum* parasites has been approached with microscopic methods by counting the number of released merozoites and following the parasitaemia subsequently. We aimed to study the reinvasion from a metabolic viewpoint, i.e. macroscopically, by measuring the lactate production of infected red blood cell cultures over two subsequent life cycles. Mathematical equations describing the lactate production of uninfected and infected red blood cells in terms of the change in parasitic biomass over time were used to obtain a reinvasion model. The model was fitted to experimental data to identify unknown parameters like the reinvasion efficiency factor. Subsequently the average number of merozoites was calculated with an average of 16 ± 4, in agreement with literature findings. Using the lactate production to study the reinvasion is a complete new approach and is advantageous as the whole cultures are studied in stead of a few hundred cells under microscopes and we gain mechanistic insight into the process. The model can now be used further to study the impact of various factors on the reinvasion more quantitatively.

Abstract

Modelling of reinvasion efficiency in *Plasmodium falciparum* cultures

M. M. Oosthuizen

Department of Biochemistry
University of Stellenbosch,
Private Bag X1, Matieland 7602, South Africa.

Thesis: MSc BSc Biochemistry

March 2017

Die virulensie en felheid van 'n malaria infeksie in 'n menslike gasheer is afhanklik van hoe effektief dogter merozoïte rooibloedselle binnedring. Kwantitatiewe insigte oor die effektiwiteit van indringing van die *P.falciparum*-parasiete tydens bloedfases is nog baie beperk. Voorheen is hierdie probleem benader deur van mikroskopiemetodes gebruik te maak om die aantal ontwikkelende merozoïte te tel en die gevolglike toename in parasetemie te volg. Die fokus van hierdie studie was om parasietindringing makroskopies te bestudeer van uit 'n metaboliese oogpunt, deur die laktaatproduksie van ongeïnfekteerde en geïnfekteerde rooibloedselle beskryf in terme van die verandering in parasitiese biomassa met verloop van tyd. Die model is instaat daartoe om eksperimentele data te gebruik om onbekende parameters, soos die faktor van herindringingsdoeltreffendheid te identifiseer. Daarna is die gemiddelde aantal merozoïte berekend met 'n gemiddeld van 16 ± 4, wat deur literatuurbevindings ondersteun word. Deur die laktaatproduksie te bestudeer is 'n totaal nuwe benadering tot die onderwerp gevolg. 'n Studie van heelkulture, in plaas van slegs 'n paar honderd selle onder 'n mikroskoop laat ons toe om 'n beter meganistiese insig oor herindringing te bekom. Die model kan nou gebruik word om die impak van verskeie faktore op herindringing meer kwantitatief te bestudeer.

Acknowledgements

I am overwhelmed with gratitude as I submit this thesis, I would like to thank the following people and organisations:

- amazing supervisors, Prof. Jacky Snoep and Dawie van Niekerk. Thank you for your patience and kind guidance, I learned so much from you,
- The South African Research Chairs Initiative (SARChI) for without funding it would not have been possible,
- Johann Eicher, Kathleen Green, Carl Christensen and the rest of the friends in the MSB-lab,
- friends and family for amazing support, food and enormous amounts of coffee,
- my parents for constant support and encouragement,
- my Father for unconditional love, strength and purpose

Dedications

Hierdie tesis word opgedra aan my grootouers, Pieter en Marlene Groenewald, en ouers, Christoffel en Petrie Oosthuizen, dankie vir jare se liefde en ondersteuning.

Contents

List of Figures

List of Tables

Nomenclature

CP	centriolar plaques
CM	culture media
CDKS	cyclin-dependant kinases
EM	electron microscopy
GAPDH	glyceraldehyde-3-phosphate dehydrogenase
HbE/EE	Hemoglobin E disease
SA	Hemoglobin S heterozygous
SS	Hemoglobin S homozygous
LDH	L-Lactate Dehydrogenase (E.C. 1.1.1.27)
MCA	Metabolic control analysis
MTOCs	microtubule organizing centres
NIMA	Never in mitosis gene A kinases
NPPs	new permeability pathways
Neks	NIMA related kinases
NAD^+	Oxidised Nicotinamide adenine dinucleotide
PHT1	parasite hexose transporter
RBC	parasitized red blood cell
PFK	phosphofructokinase
pmi	post merozoite invasion

PK	pyruvate kinase
SCD	sickle cell disease
SPBs	spindle pole bodies
uRBC	uninfected red blood cell

Chapter 1

Introduction

Malaria is a disease that has caused millions of deaths, and although progress has been made in decreasing mortality rates and the number of people at risk of infection [1], we still don't completely understand the biology of the life cycle. This inhibits effective drug development against the parasite, which is becoming increasingly resistant to current prophylaxis and treatment.

Upsurge of drug resistance and history of drugs Environmental conditions, economic changes and social conditions lead to occasional breakdown in malaria control that advance new resistance and subsequently epidemics [2–4]. Artemisinin resistance in *Plasmodium falciparum* is confirmed in Western Cambodia, the border of Thailand and Myanmar [4, 5]. The development of resistance in these areas is of great concern especially as resistance against chloroquine and sulfadoxine-pyrimethamin originated there [4, 5]. The resistance was able to spread to Asia and Africa which lead to a great setback in current progress to eradicate the disease [1, 2]. Currently there is no vaccine available for public use and resistance against the artemisinin class of antimalarial drugs is growing [6, 7].

In malaria patients, clinical symptoms that emerge are anaemia, lactic acidosis, fever, hypoglycaemia and neurological pathologies [2, 8]. A major cause of morbidity and possible mortality is anaemia [2]. This is particularly evident in cases of malnourishment, pre-existing anaemia or co-infections increasing immunological burden on the host [2].

Malaria is caused by protozoans of the *Plasmodium* genus. There are five parasite species that are able to infect, live and multiply within human red blood cells - *P. falciparum, P. vivax, P. ovale, P. malariae and P. knowlesi* [1, 9]. *P. falciparum* is responsible for most fatalities in humans and is the most abundant malaria parasite in sub-Saharan Africa [1]. The complex *P. falciparum* life cycle spans over stages in the vector (female *Anopheles* mosquito) and the human host. The host is infected with sporozoites during a blood meal through the saliva of the *Plasmodium* infected vector. After the host is infected, the parasites move to the liver cells (hepatocytes), where, after multiple rounds of mitosis, thousands of merozoites are released by the infected hepatocytes. Following this, the merozoites move into the bloodstream and

the intraerythrocytic phase starts. The parasite begins a 48 hour reproduction cycle during which the merozoites enter the erythrocytes by a four step invasion process [2] where after the merozoite changes into a thin discoid, cup-shaped ring. The merozoite grows exponentially, differentiating into the ring-shape $(0 - 24h)$, to a trophozoite $(24 - 36h)$ [10] and a schizont $(36 - 48h)$ [10].

It is during the last $14h$ of the life cycle that the cell replicates the genetic material to release the daughter merozoites when the schizont bursts at $48h$. In *Plasmodium* asynchronous division occurs that leads to a multi-nucleated syncytial host cell. The division is regulated by processes less well understood despite the evolutionary conserved cell regulation by cycle kinases and phosphatases [9]. The asynchronous division of *P. falciparum* leads to a number of merozoites that currently appears to vary greatly within cultures [9]. These merozoites are released into the blood stream, and a fraction of them reinvade a new RBC to enter the next cycle. This process of merozoite release and subsequent reinvasion, has not been analysed extensively.

The number of merozoites released influence the parasite multiplication rate, which has a direct influence on growth rates and virulence [10]. The reinvasion is a crucial step for the survival of the parasite it is therefore also a good target for drugs [7]. A basic understanding of the kinetics of parasitic growth and multiplication is very important for development of pharmaceutical intervention such as anti-merozoite vaccines and novel invasion-inhibitory compounds [7].

As biochemical analyses of the insect stages and intra-hepatocytic cycles are challenging and the symptoms of malaria infection are strongly associated with the blood stages, research has focussed more on the blood stages [9]. During the intra-erythrocytic stages of the *P. falciparum* life cycle, the parasitized red blood cells (pRBCs) have an increased metabolic activity of about 60 to a $100\times$ that of uninfected red blood cells (uRBCs) [11]. This is due to the fact that the parasite depends completely on glycolysis for all its energy requirements and has a fast growth rate. The increase in lactate in the blood can lead to lactic acidosis which is often seen in severe malaria patients [12]. Lactic acidosis is the state where lactate builds up in the blood to concentrations $> 5mM$ and the pH in the blood decreases [13]. Mehta et. al [14, 15] found that the uRBCs in the environment of pRBCs could also experience metabolic inhibition.

Penkler [16] constructed a mathematical model that describes the whole glycolytic pathway of *P. falciparum*. This model enables us to study various enzymes as drug targets and the effect of targeting a specific enzyme on metabolic flux. Du Toit [11] went further and linked Penkler's [16] with Mulquiney's [17] RBC model. He also studied the growth of the parasite and showed that the lactate production rate stays constant per parasitic biomass volume. We would therefore expect that lactate production should increase exponentially over multiple 48 hour cycles. At every reinvasion event however, the rate of lactate production changes. If the lactate production rate stays constant per volume biomass we must conclude that the change in rate of lactate production is caused by the change in biomass at every reinvasion event. Analysing the experimental data with this mathematical model allows us

to gain insight into the growth behaviour of the parasite. What is specifically of interest for this study, is the merozoite production and release, reinvasion into new RBCs and the metabolic activity during this event.

The research questions that emerged were: i) Is it possible to use simple exponential equations as a phenomenological model to describe the lactate production over parasitic life cycles to study the reinvasion efficiency? ii) What is the contribution of uRBC lactate production in the system and how is it influenced in the presence of growing parasites? iii) Can we construct a mechanistic model that describes the lactate production of a culture-like system based on the changes in biomass that occur during the reinvasion process? Since reinvasion is critically important to the reproduction of the malaria parasite, we aim to answer the research questions above and give a quantitative description of this process.

The aim of the thesis is therefore to give a quantitative description of the reinvasion process. The approach we used for this is based on iteration between experiment and mathematical modelling. The following iterations were used and are objectives for the study.

- Describe the lactate production by the parasites and the uRBCs, individually with a phenomenological model
- Quantify the observed inhibition that the parasites have on the uRBCs glycolytic activity
- Construct a mechanistic model to describe the lactate production of the system over two 48 h parasitic life cycles
- Test the model's ability to predict the lactate production with experimentally determined parameters
- Fit the mechanistic model to experimental data to obtain new values for parameters (such as the reinvasion efficiency)
- Calculate the average number merozoites produced by the schizonts in the experimental incubation using the fitted model results and microscopical data

By achieving these objectives we will be able to answer the research questions, understand the reinvasion and reproduction of the *P.falciparum* parasite better, and gain insight into the metabolic effects on the uRBCs in the presence of iRBC.

Chapter 2

Literature Study

2.1 Introduction

Statistics and history of the disease According to the WHO Malaria Report 2014, malaria is the world's most infectious disease. In 2013 there were 198 million cases and 584000 deaths. The heaviest burden is in the African region, where 90% of the deaths occurred with 78% being children under the age of 5 [1]. Although infection decreased by 47% globally between 2000-2013, 1.2 billion people are still at risk [1].

The protozoan disease is caused by five parasite species of *Plasmodium* genus that infect human red blood cells namely, *P. falciparum, P. vivax, P. ovale, P. malariae and P. knowlesi* [1, 9]. *P. falciparum* reigns in the sub-Saharan African areas and is responsible for the most fatal malaria cases [1]. The clinical symptoms of malaria: fever, lactic acidosis, anaemia, hypoglycaemia and neurological pathologies, relate to the blood stage of the parasite cycle [8]. The disease is curable but the development of resistance to 4-aminoquinolones, resulted in replacing treatment with artemisinin [18]. Unfortunately resistance against artemisinin-based drugs is now found worldwide [18]. Thus over the last few years alternative approaches are being sought.

The parasite has a complex life cycle that occurs within a mosquito vector and human host. Malaria is transmitted through the female *Anopheles* mosquito to a host during a blood meal. The sporozoites inhabit the liver hepatocytes where the parasites multiply extensively through mitotic nuclear divisions to produce up to 30 000 merozoites [19]. After about 2-3 weeks of infection the hepatocytes burst open and the merozoites enter the bloodstream where red blood cells (RBCs) are invaded. After a full life cycle (48 hours) the parasitized red blood cell (pRBC), containing a multi-nucleated schizont, bursts open to release merozoites, some of which reinvade RBCs to repeat the cycle.[19]

The DNA replication of the parasite is asynchronous leading to a range of between 8-30 merozoites[10]. These merozoites are released to enter RBCs. The process of reinvasion is not an easy task as multiple factors are acting against the entrance

of the merozoite : very specific receptor - ligand interactions, motile response and the short half-life of the merozoite [20]. Since so many factors are involved in both merozoite production and the reinvasion event, it is difficult to model these processes quantitatively, and we are still uncertain on the kinetics of this process.

When specifically focussing on the nutrients and metabolism, the situation where one eukaryotic cell is living inside another presents unusual challenges as the erythrocyte is biochemically less active than the parasite [21]. To obtain enough resources the parasite needs nutrients from the extracellular environment and the rate of consumption by the parasite exceeds the rate of consumption of an uninfected host cell [21]. The *P. falciparum* parasite completely relies on glycolysis for energy production from glucose transported over the membrane. When the parasite reaches mature trophozoite stage, the glucose uptake and utilisation rate can reach up to 100 times that of its host RBC [22]. The increased lactate flux into the blood stream is thought to contribute to the state of hypoglycaemia and lactic acidosis which are key indicators for poor chances of survival [11].

This chapter will discuss background information relevant to the content of this study with the focus on the biology of *Plasmodium falciparum*.

2.2 Life cycle of *Plasmodium falciparum*

Merozoites start a 48 hour reproduction cycle by invading the host's erythrocytes. The merozoites are encapsulated by the erythrocyte membrane through a complicated invasion process. After invasion the merozoite starts growing and differentiates into a thin discoid, cup shaped ring [23]. The merozoite then starts to import haemoglobin as a source of amino acids needed for growth [24]. The parasite is in ring-shape from $(0-24h)$ and $14h$ into the parasite's intracellular cycle the mitotic processes for DNA replication is initiated to undergo 3-4 rounds of DNA replication. From $(24-36h)$ it matures from a young trophozoite to a mature trophozoite [10]. The parasite then differentiates further into a schizont $(36-48h)$. Chromosome replication continues till $42-44h$ pmi with nuclear bodies forming foci around the digestive vacuole in preparation for merozoite formation in the latter stages of shizogony. The foci are responsible for arranging the nucleus, plastids, mitochondrion, and other cellular components necessary for the production of the mature merozoites before merozoite are released at around $42-48h$ pmi.[23] At this point the parasite is a synctial schizont ready to release up to 30 merozoites. The erythrocyte undergoes lysis at $48h$ to release the merozoites into the bloodstream as an eruptive event [16, 19, 25, 26].

Literature holds diverse opinions and models on the production and release of merozoites at the end of the erythrocytic cycle [27, 28]. The population is able to multiply up to 20 times per cycle [2]. As the prospect of this study is to quantify the complex process of merozoite production and reinvasion, we will now focus on DNA replication in order to understand merozoite production and the dynamics of the invasion process.

2.2.1 DNA replication and merozoite production

Arnot et al.[9] studied the appearance, movement and division of *P. falciparum* nuclei and mitotic organizers during shizogony and compared it to eukaryotic cell division.

Mitosis can, broadly speaking, be divided in to *open* and *closed* mitosis. In higher eukaryotes *open* mitosis is more frequently observed in which disintegration of the nuclear envelope follows chromosome replication and only reforms after chromosome segregation. The spindle microtubules then emanate from the extra nuclear centrosomes to draw the replicated chromosomes in opposite directions [29]. *Closed* mitosis however, occur in yeast where the mitotic spindle is initiated within an intact nuclear envelope [29]. Centrosomes are not present but the mitotic spindle is generated from spindle pole bodies, lacking centrioles in the nuclear membrane [29]. The chromosomes are drawn to the opposite nucleus poles after which it divides by fission producing two daughter nuclei within a cell before it divides [29].

P.falciparum mitosis appears to be a combination of *closed* mitosis seen in yeasts, as well as aspects of the paired centriolar divisions of centrosomes in the eukaryotic *open* mitosis [9]. The parasite's nuclear envelope membrane contains microtubule organizing centres and are essential in organizing which interactions can occur, which is characteristic of *closed* systems also termed *crytomitosis* in older literature.

Microtubule organizing centres are electron dense, complex structures such as centriolar plaques, kinetic centres, centrosome equivalents in mammalian cells or spindle bodies in fission centrioles [30] that are important for nucleation and organizing microtubule arrays. They may occur in a diversity of complex conformations present in the cytoplasm or found embedded within membranes [31, 32]. *P.falciparum* spindle microtubules originate from the nuclear envelope-embedded structures and stay attached throughout mitosis that resembles yeast spindle pole bodies [9], but also contain centrioles within intact nuclear membranes shown by Akaiwa and Beaudoin [33]. It is sometimes referred to as centriolar plaques or even just spindle pole bodies when structural differences are downplayed [34]. Centrosomes duplicate at the start of cell division to form parallel cylindrical structures at the edge of the nuclear membrane, which then split. During the S phase, daughter centrioles realign perpendicular to each side of the parent centrioles and elongate. [29] This triait is shared by SPBs and *P.falciparum* thus combines characteristics of both *open* and *closed* systems to preserve the nuclear membrane with eukaryotic centriolar division process [29].

The results of DNA replication studies by Arnot et. al [9] clearly favours a S /M /S /M /S /M type phase progression. During the first M phase, the first duplicated chromosomes separate into the dividing nuclear body, each inheriting a mother and daughter centriolar plaque after which a pre-S and G1 gap is returned [9, 29]. In conventional non-syncytial mitosis, cell division would follow, but instead the daughter nuclei re-enters the S phase and divide again. As the second round division results in daughter nuclei inheriting a mother CP and the other a daughter CP, the mother

CP progresses faster so that mitotic division is not synchronous [29, 33]. After the second round of division cycles, the new daughter nuclei divide quasi-independently resulting in asynchronous nuclear stages each with its own division processes and early schizonts with odd numbers of daughter nuclei [9, 29]. Multi-nuclear cells are observed as part of the reproductive strategy in *P. falciparum* [35, 36]. When compared to fibroblast, standard yeast and multicellular embryo models, there are also several marked differences. In other multi-nucleated systems, like insect embryonic syncytia, the nuclei divide synchronously where in *P. falciparum* chromosome replication is not immediately followed by nuclear division and cell division [29].

Regulators The DNA replication regulation seems minimal, as after the first division, the rest of the division cycles operate with a degree of dependence on a specific daughter merozoite's readiness of centrisomal components [29, 37]. Each daughter merozoite being independent from the other.

An interesting observation made by Arnot et al. [29] was that the last schizont division appears more in phase. This suggest that mitotic checkpoints could be involved allowing lagging nuclei to catch up by rapid assembly of nuclei and organelles into the merozoites [36]. This enables unified movement of nuclei to merozoite buds prior to schizont or RBC rupture [9, 29, 38].

Regulatory proteins that have been identified are *Plasmodium* protein homologues of known cell cycle regulatory proteins. These include cyclin-dependant kinases, never in mitosis gene A kinases (NIMA), centrin proteins and Aurora-related kinases with various *Plasmodium* species [30, 39–43]. NIMA - related kinases (Neks) are encoded by two *Plasmodium* genes that do not have a defined cell cycle role. Reininger et al. [43, 44] found that nek-2 and nek-4 are not neccesary for mitosis in intra-erythrocytic development of the parasite while studies on nek-1 and nek-3 suggested that they are essential in this stage [45]. The regulation of mitosis therefore differs from standard eukaryotic models of diffusing waves of cyclin and cyclin dependant kinases that control the synchronised cell cycles. Equivalents of higher eukaryotic cellular structures can however be seen from electron microscopy, [9, 33, 38] which shows traits of standard eukaryotic models.

If the replication and division occurred in a fully synchronised manner as expected from binary divisions, a geometric number of daughter merozoites would be produced [8, 9]. The multi-nuclear cell, however, leads to asynchronous duplication and independent nuclear division of nuclei [9] and in turn produces even and odd numbers of daughter merozoites beyond simple geometric progression as observed by Reilly et al. [10].

2.2.2 Reinvasion

At the end of the life cycle, between 8 and 30 spherical daughter merozoites are produced with a size of about $1.5\mu m$ in diameter and an apical tip [46, 47]. The apical tip is important for motility and driving the parasite into host cells, which

makes the merozoite very well adapted for its task of finding and invading host cells [36].

The egress of the merozoites is triggered by low environmental potassium levels that activates a cytosolic calcium increase [47]. The merozoites are released in an explosive like event [25] after which they travel with random movements in search of a susceptible RBC. In these fleeting minutes before the merozoite is safe inside a RBC, the merozoites are most vulnerable to the host defences [47]. An antibody response to various antigens of the merozoites is initiated, so much so that Gamma globulins have previously been harvested from malaria immune individuals to treat non- or partially immune children [47, 48]. Another challenge for successful reinvasion is the short half life of about five minutes in $37°C$, as the invasive potential of merozoites decrease rapidly and they are removed from circulation by phagocytic cells [46, 49, 50]. At room temperature the half life is about 15 minutes, where as if the temperature increases to $40°C$ the half life decreases to about 2.5 minutes [49].

If the merozoite finds a susceptible RBC, reinvasion starts in a step-like manner, showing a possible dependency on triggers such as receptor-ligand interactions to continue to the next process [7, 47, 51]. The pre-invasion process proves to be one of the biggest factors influencing the reinvasion efficiency. The receptor-ligand interactions play a critical role in the pre-invasion process and appears to be conserved between the two *Plasmodium* strains, *P.knowlesi* and *P.falciparum* [52–54].

The first recognition between the merozoite and the RBC is a weak interaction over relatively long distances and is still reversible [55]. The surface proteins of the merozoites are secreted at specific times and play an important role in adhesion and motility [36]. Primary attachments of the polar merozoite appears to involve the surface proteins and the RBC, after which the RBC deformations starts. This is activated by calcium from the parasite and necessary for the reorientation of the merozoite for apical alignment [47]. Dvorak [52] and Glushakova [56] observed changes in the shape of the RBC under invasion attack by a merozoite termed as the motile response. The movements stop after $10 - 30$ seconds and the RBC returns to its original shape [54]. Although Striepen et al. [36] is of the opinion that the motile response does not have an impact on the reinvasion efficiency; Lew et al. [54] states that a poor motile response of the RBC has a negative impact on the success of apical alignment and the efficiency of invasion. The invasion efficiency will decrease in several RBC abnormalities like RBC hydration, haemoglobin, cytoskeleton, membrane lipid composition, metabolism or membrane transport generating a deficient motile response [57, 58]. When the merozoite and RBC is aligned apically, the merozoite binds irreversibly to the RBC surface through its rhoptry proteins and microneme proteins as a tight junction with electron dense circumferential apposition. The merozoite starts invading the RBC with the help of its internal actin-myosin motor [7, 36, 47, 51] and the junction moves from the apical point to the posterior end as the surface proteins of the merozoites are shed [7, 46, 47, 51].

When the merozoite reaches a RBC and invasion is initiated successfully, the invasion process is very quick and happens within a few seconds, causing minimal disruptions

to the host cell [36].

2.3 Quantification of reinvasion efficiency

The term reinvasion efficiency refers to the percentage of merozoites released by the average schizont that successfully re-enter RBCs to continue into the next cycle. It therefore requires both the quantification of the merozoite production in shizogony and the quantification of reinvasion. Boyle et al. [7] notes that the precise mechanism describing how the merozoite re-enters a RBC is still not fully understood due to the technical difficulties in studying merozoites. There are multiple factors that influence the success of the reinvasion and it is therefore not a simple process to quantify mathematically. Other studies on the replication and reinvasion on *Plasmodium knowlesi* have been more successful which gave insight on the invasion kinetics [59, 60].

2.3.1 Factors that influence reinvasion efficiency

Several factors that influence reinvasion efficiency such as receptor-ligand interactions, merozoite half-life and the motile response have been mentioned in the previous section. There are however other factors that also contribute to reinvasion efficiency such as metabolic triggers and the susceptibility of RBCs (dynamics within the blood stream, the age class and RBC pathologies) which will be discussed in more detail below.

Metabolic triggers The intra-erythrocytic metabolism of the parasite, fulfil more than just the need for ATP [61]. It has adapted to cells that need to proliferate rapidly. These adaptations include deregulated glycolytic activity coupled with impaired mitochondrial metabolism to generate intermediate essentials for rapid biomass generation for schizogony [61]. Various studies have confirmed that due to the parasite's access to the host RBC hemoglobin, it has most of what it needs but is still dependant on various external metabolites and amino acids like iso-leucine for parasitic growth [61]. Reilly et al. [10] noticed a decrease in PMR (parasite multiplication rate) between the first and second cycle, with cultures starting at 0.1% *par*, 5% Hematocrit and suggest that it is due to deteriorating media quality and limited resources. It was confirmed by Salcedo et al. [61] that stress conditions *in vitro* and *in vivo* cause the parasite to have different responses in terms of life cycle commitment. This leads to possible changes in the proliferation and egress phenotype via one of the metabolites [61]. It is still not clear, however, if this means that the parasite compromises on the number of merozoites produced or a slower cycle time as both these factors influence the PMR.

The cellular metabolism of malaria parasites under variable nutrient availability is still poorly investigated [61] and it is necessary to better understand the proliferation in light of the parasitic metabolism. Using standard culturing conditions, Ferrer et al. [26] found that under the usual experimental conditions, glucose and lactate concentrations or diffusion limitations thereof, does not limit global behaviour. The

observed thresholds for the reinvasion in static cultures were the spreading of merozoites and the susceptibility of RBCs.

Bloodstream dynamics Within the bloodstream the merozoite needs to overcome high tension in a forcefully moving environment, the flux of O_2 and frequent passage through the spleen in order to successfully invade a RBC [62]. Lewis et al. [54] noted a decrease in invasion efficiency with decreasing RBC density probably due to a reduced number of RBCs that are close enough, uninfected and available for invasion. The moment the merozoite is safely inside, the RBC is a very advantageous host cell as it lacks their own microbicidal apparatus and protection against contact with antibodies [62].

RBC age classes The idea that RBCs' susceptibility to merozoites changes with their age classes has been proposed by a few authors [63–65]. This preference to a specific age class will lead to a limited selection of RBC available for merozoites to invade and therefore increased competitions between merozoites for a host RBC. In an attempt to quantify the reinvasion event, Ferrer et al. [26] employed the probability of infection as a characteristic of the individual RBC that reduce both with age and time in culture [66]. Kerlin et al. [67] states that during *P.falciparum* infection a wider range of RBC age classes are infected with merozoites, leading to an overall reduction in RBCs and not a specific age class. Both Barnwell [68] and Harvey et al. [47] agrees that *P.falciparum* has the capacity to invade erythrocytes of all ages. For the current study the preferential RBC invasion is assumed not to be a factor contributing to the efficiency of the reinvasion.

RBC pathologies Examples of RBC pathologies include sickle cell disease (SCD) and Hemoglobin E disease (HbE/EE) patients. Upon deoxygenation the hemoglobin S homozygous (SS) and hemoglobin S heterozygous (SA) erythrocytes are distorted to sickle cell shape leading to abnormal characteristics of the viscosity, membrane contents and metabolic intermediate concentrations which leads to an unfavourable environment for *P.falciparum* growth and a decreased disease severity is observed [69]. With the reversible state of HbS for the resistance of the disease in SA and SS, a slower growth rate also accompany HbE RBCs, a mutant carried by about 30 million people in Laos, Thailand, South-east-Asia, Cambodia and up to 55% of people in and around Samrim and the ancient temple [70] and EE patients are less capable of sustaining the growth of *P. falciparum* [70].

2.3.2 Current methods

In attempt to study and quantify the merozoite production and reinvasion current methods depend on microscopes and high speed digital cameras [47]. This consist mostly of microscopy work such as electron microscopy (EM), Fluorescent light microscopy, light microscopy, confocal laser scanning microscopy with fluorescence in sito hibridization (FISH), live video capturing and semi-high through put growth assays with radio labelled Hypoxanthine.

EM has been used for decades to understand major sequence events in the nuclear development of *Plasmodium* parasites such as the DNA replication, and has produced the best simultaneous views of MTOC duplication, mitotic spindle assembly and chromosome segregation. The great resolution (0.2 nm) of TEM even revealed individual microtubules of the mitotic spindle [38, 71, 72]. EM was used to describe the alignment of new budding nuclei at the edge of the schizont, the daughter organelles assembling at the opposite spindle poles, and the start of cytokinesis around the new nuclei [31, 71, 73]. Fluorescent light microscopy continues to be a great asset in research on *P. falciparum's* mitosis and it complements data gathered from TEM [9, 30, 73, 74].

An advantage that light microscopy has on TEM is less-disruptive fixation conditions with less susceptibility to various artefacts as well as the opportunity to see organelles in living cells [75] with several markers that correlate with the development within the nuclear cycle [73, 76]. Light microscopy has been and still continues to be integral to malaria research. Relevant to the current study, it was used by Reilly et al. [10] to study schizonts by counting the number of merozoites in each. Reilly [10] studied the growth and proliferation using blood smears and hypoxanthine incorporation. They examined several nested steps of growth including cell cycle progression and duration, merozoite production and re-invasion efficiency [10]. Parasitaemia was determined and fold change for each life-cycle was calculated [10].

Using a counting study, Reilly et al. [10] concluded that an average of 16 merozoites were produced per schizont with an average parasitic life cycle time of 49.7 hours. Reilly et al. [10] also observed a maximum reinvasion efficiency for their experiments of about 25% which was influenced by RBC density and starting parasitaemia [10]. They confirmed the outcome of asynchronous DNA replication, as the arithmetic of daughter merozoites (8 to 30) are not limited to geometric numbers [9, 10]. The number of merozoites produced would even vary 2- to 3-fold within clonal *P. falciparum* cultures growing *in vitro*. [77, 78]. This denotes that a fixed number of nascent nuclei is not required for progression to cytokinesis [8].

Arnot et al. [9] studied cell division cycles with the use of FISH. This is another method which provided valuable insights using semi-high through put growth assays with radio labelled hypoxanthine which is a nucleic acid precursor acting as a reporter of whole cycle proliferation [10].

A theoretical attempt to quantify the reinvasion event by Ferrer et al. [26] predict 8, 16 or 32 merozoites to be released from an infected RBC after its $48h$ life cycle. Unfortunately their approach does not account for asynchronous merozoite production, or the effect of the short half life of merozoites. Pasvol et al. studied the probability of infection as a characteristic of the individual RBC that reduce both with age and time in culture [66].

Amongst others from literature who quantified the reinvasion, Kerlin et al. [67] used a scaling factor of 0.7 as the maximum fraction of merozoites released that will survive the reinvasion event and develop in a new RBC within the native host. Boyle

et al. [49] noticed that the invasion efficiency is dependent on merozoite to uRBC ratio and that a decrease in the ratio (excess uRBCs) leads to increased reinvasion rates. They also saw an independent increase on invasion rate when increasing the hematocrit (RBC concentrations of 113, 226, $340\times10^3/\mu l$ = reinvasion rates of 7.1, 7.7, 8.8% respectively). Boyle et al. [49] found that with the use of their filtration method, isolated merozoites could reinvade with efficiencies of 17.7%, 16.5% and 14,9%. They calculated the reinvasion efficiency in *in vitro* cultures and estimated it to be 20-40% based on the assumption that 16 merozoites will be released per schizont and a 4-7 fold replication per cycle.

The number of merozoites produced by asynchronous division are beyond simple geometric progression. This complicates the prediction of a single number of merozoites produced by a schizont. In addition, each of the above mentioned factors could play a role in the success of the reinvasion. As non of these have been quantified, we again notice the lack in current insight on the quantification of the whole reinvasion event from schizogony to successfully reinvaded parasites.

2.4 *P. falciparum* metabolism in Erythrocytes

After the parasite infects the host RBC, a shift in metabolic activity of the RBC is observed. The parasite does not have any carbohydrate reserves, but has access to the nutrient rich cytosol and obtains its glucose resources from the host RBC's cytosol. Glucose is now utilized up to 100 times faster by the RBC. Several enzymes in the glycolytic pathway of pRBCs are activated [79] whilst the metabolic activity of the host RBC is inhibited [14, 15]. Glucose is transported into the cytosol via the endogenous hexose transporters as well as the new permeability pathways (NPPs) [80] appearing in the RBC membrane between $12-16h$ pmi. These channels are non-specific channels that allow the transport of nutrients into the host RBC [81]. Glucose is then transported over the parasite plasma membrane through the parasitophorous vacuole membrane, a non-selective, high capacity channel [81] through the parasite hexose transporter (PHT1) [82].

The pRBC rapidly consumes glucose and utilises it via the Embden-Meyerhof pathway. The stoichiometric production and accumulation of lactate confirms earlier accounts of the lack of a functional Krebs (TCA) cycle in both the host RBC and the pRBC. The parasite is therefore dependent on glycolysis for all its energy requirements.

2.4.1 Inhibition of erythrocyte metabolism

Changes occur as growing parasites inhabit the host RBC. Various proteins have been detected to be exported from the parasite to the RBC cytosol namely kinases, lipases, proteases, adhesins and chaperone-like proteins. The RBC membrane loses a degree of flexibility, and obtains increased permeability to low molecular weight solutes [83]. This is due to NPPs that appear in the RBC membrane at 12-16 hours post invasion as mentioned earlier [81]. The volume of the parasite expands 15-20

fold after infection within the RBC host, suggesting that mechanisms should be in place to regulate the osmotic balance of the pRBC. This is also where the NPPs could possibly be crucial for the volume control of the pRBC and the survival of the parasite [80].

According to Mehta et al. [14, 15] uRBCs convert 90% of glucose to lactate, whereas growing parasites have a glucose to excreted lactate yield of only 60-70% [84]. The rest of the glucose serves as a source of carbons for biomass production as nucleic acids, glycosylated proteins and lipids that are crucial for parasite growth [14, 15].

Recent research found that the metabolic activity of uRBCs is down-regulated in the presence of growing parasites in pRBCs [11, 14, 15]. Metha et al. [15] proposed that it is due to the combined effect of a drop in pH, increasing amounts of lactate and yet to be identified, metabolic compounds.

Initial studies were performed, by allowing synchronised cultures to grow for $17 - 20h$. The supernatant was used as conditioned media and glucose utilization and the glycolytic intermediate, 2,3-diphosphoglycerate was measured [14]. The results showed glucose utilization inhibition ranging between 28% and 81% [14]. Mehta et. al [15] further studied the isolated effect of pH and external lactate concentrations and the combined effect at 20 mM lactate. They observed that pH does have a significant effect on the metabolic activity of normal uRBC [15]. Inhibition due to external lactate was not accounted for as they found it to be negligibly small.

The influence of pH on the activity of two metabolically irreversible enzymes (PFK and PF) were studied, and it was demonstrated that pH inhibits host phosphofructokinase (PFK) but not pyruvate kinase (PK) enzyme activities. Enzyme specific assays were performed to investigate the mechanism of inhibition by the culture media (CM) on PFK, PK, G6PDH, three of the ezymes involved with glucose metabolism [15].

Mehta et. al [14] demonstrated that a decrease in pH selectively inhibits the host PFK, but not PK enzyme activity. This could still not be responsible for the extent of the decreased metabolic activity [14]. The inhibitory effect on the metabolic flux of the uRBC subsequently has a direct influence on any metabolic studies. The quantification thereof is thus very relevant for our *in vitro* metabolic studies of parasitized RBC cultures.

2.5 Systems biology

Systems Biology studies the functional relationship between components of a system to understand how properties of the whole system arise from these components or and their interactions [85]. In order to achieve this, experimental research on molecular level and cellular level are required. It is a fast developing discipline that combines biology with different sciences namely physics, ecology, mathematics and chemistry [85].

Systems Biology has proven its worth in leading to many new scientific insights and the potential of becoming part of mainstream biology is starting to unfold rapidly. It has become evident that there are some properties of systems that can be understood only when different levels or components of systems are studied together [85].

At the core of Systems Biology is the use of mathematical models. A mathematical model consists of equations and functions that characterise the relationships between variables. In Systems Biology models have been used to describe diverse phenomena both in the natural and social sciences, but mostly by physicists, computer scientists, engineers, and economists [11]. Models aim to describe large scale populations and whole systems, organisms, cells or metabolic networks.

Metabolic models Metabolism is an attractive system to model to find out which enzyme could serve as a credible drug target by quantifying the effect that inhibition of individual enzymes have on properties of the system as a whole [16]. Relevant to the current study, it is known that intraerythrocyte parasites do not have any other source of energy than ATP from glycolysis, gained through its access to the hosts cytosol [16, 22].

Penkler [16] characterised the glycolytic enzymes of the *P.falciparum* in the trophozoite phase and constructed a glycolytic model with a bottom-up approach. For each of the enzymes a rate equation was constructed that describes the kinetic behaviour of the individual enzyme in terms of enzyme specific parameters obtained from experimental data.

The validated model provided a tool for drug target identification in *P.falciparum* glycolysis. Metabolic control analysis (MCA) is a method of analysis currently used in Systems Biology. It is used to characterise the control that a specific enzyme has on the flux through the system and subsequently used to identify enzymes to be targeted for drugs. The glucose transporter, PfHT1, was identified as having high control on the parasite's glycolytic flux, but low control on the host erythrocyte flux [16]. This confirmed the concept that it is far more efficient to identify a drug target in context of the whole system instead of breaking the system up and studying each of the components separately until a target is discovered[16].

Du Toit [11] constructed a multi-compartmental mathematical model for glycolysis of the malaria parasite *P. falciparum* inhabiting erythrocytes by combining previously constructed and validated kinetic models of the parasite [16] and the erythrocyte [17]. He successfully elucidated the mechanism behind the system's response to extracellular glucose perturbations. An inhibition mechanism for the glucose transporter was included to make predictions of the effect of an inhibitor over a range of external glucose concentrations which could be useful for analysing drug inhibitory effects.

Du Toit [11] studied the growth of the *P.falciparum* parasite during one cyle of 48 hours in the blood stage and used the change in volume to expand Penkler's [16] model to predict the glycolytic activity during each of the intra-erythrocytic

life cycle assuming non-differential enzyme expression. Validation of the model confirms that the activity during the various life stages in a RBC could be described with reasonable accuracy using the model [11]. The current model can predict the lactate production during one life cycle (48 hours) of the parasite fairly accurately. The effect that pRBCs have on the metabolic activity of uRBC during the parasitic intraerythrocytic life cycle is as yet not kinetically quantified and incorporated into the model. With Du Toit's[11] model, predictions of higher-level systems behaviour could be presented based on characterised and validated lower-level components. By including the reinvasion efficiency and number of merozoites into the life cycle model simulations can be extended over more cycles [11]. The kinetics around reinvasion is therefore necessary to improve the accuracy of the model [11]. In turn, effective whole-body modelling systems will optimise research on the parasite and its detrimental effects [26].

Chapter 3

Methodology

Standard culturing conditions A strain of *P. falciparum* (D10) was cultured in T-75 culture flasks using the standard culturing conditions as described by Trager et. al [86]. The hematocrit was maintained at 3-4% with A^+ packed human erythrocytes (donated from the Western Province Blood Transfusion Service, South Africa) in supplemented RPMI culture media. Cultures were incubated at 37° C in airtight $250ml$ culture flasks gassed with Tri-mix gas ($3\%\ O_2, 4\%\ CO_2, 91\%\ N_2$). The RPMI culture medium ($10.4\,g/L$ RPMI 1640 with pH between 7.2 and 7.3), was supplemented with 0.5% m/v Albumax II(R)(Gibco, Life Technologies), 22.2 mM glucose(final concentration, 33.3 mM), 25 mM HEPES, 3 mM hypoxanthine, 25 mM sodium bicarbonate and 50 $\mu g \cdot ml^{-1}$ gentamycin (Sigma Aldrich). The culture media was prepared with Sabax Pour water (from Adock Ingram) and filtered with sterile syringe filters ($0.22\mu m$).

From freezer stocks Freezer stocks of *P.falciparum D10* infected erythrocytes (received initially from University of Cape Town, P. Smith) were thawed at room temperature. The pRBC cultures were treated with decreasing salt concentrations ($12\%, 1.8\%, 0.9\%$ NaCl) of saline solutions added drop wise. Culture media was added and thereafter changed daily and kept at standard conditions as described above.

Synchronization of *P.falciparum* cultures Cultures with parasites predominantly in ring phase ($0h - 12h$ post merozoite invasion (pmi)) were synchronised by centrifugation at $750 \times g$ for 3 minutes and treating the pellet with $10ml$ of 5% Sorbitol (Sigma Aldrich) for 5 minutes at 37°C as described by Lambros and Vandenveg [86, 87]. After centrifugation the sorbitol was aspirated, and the pellet was washed twice with culture media consisting of components described above. The synchronization was repeated before the start of each experiment.

Parasitaemia Parasitaemia was determined in thin blood smear slides, fixed with methanol. The fixed sample was stained with 5% Giemsa Stain in PBS Solution (Sigma Aldrich) for 5 minutes, rinsed and dried. The slide was studied with a *UB200I UOP Series* Biological Microscope under 100x magnification. The para-

sitaemia was calculated as the percentage parasite-infected RBCs in typically about 400 RBCs were counted.

Cell counts Cellcounts were done using a Neubauer Improved Hemocytometer under a *UB200I UOP Series* Biological Microscope with 40x magnification. The samples were diluted with 0.4% Trypan Blue solution (Sigma Aldrich).

Growth experiments Growth experiments were set up by preparing a $50ml$culture of *P. falciparum* rings with the necessary parasitaemia ($\pm 1\%$) and hematocrit ($\pm 1\%$). The culture was aliquoted over 24 smaller T-25 cultures flasks for each time point. Over a time frame of 96 hours, at 4 hour intervals, a sample was taken. The number of cells in each sample were counted, the parasitaemia calculated, after which it was spun down and the supernatant (spent culture media) was frozen away at each time point for further studies on the lactate concentration and inhibition effect on uRBCs.

Lactate concentration determination The lactate concentration of each of the supernatant samples was determined with the use of an NAD^+ and LDH (Lactate Dehydrogenase) linked enzyme assay. The assay cocktail consisted of 5 mM NAD^+, 4U LDH (Sigma Aldrich), $16\mu l/ml$ Hydrazine (Sigma Aldrich), made up in 150 mM HEPES/$MgSO_4$ Buffer ($pH = 7.6$). A series of lactate standards were prepared by making serial dilutions from 10 mM Lactate. The samples were diluted if necessary, and 5 μl sample used per well in a 96 well microtitre plate. The assay cocktail (95 μl) was added to each well and incubated for 90 min at room temperature away from light. The absorbance values were measured with a VarioSkan microplate reader (Thermo Electron Corporation) at 340nm pre-heated to 37° C. The lactate concentration of each of the samples was finally calculated by comparison to the standard curve.

Inhibition studies The effects of pH and lactate concentrations on the metabolic activity of the uRBCs was determined by incubating the uRBCs in culture media in a 1:1 volume ratio with a range of pH values and lactate concentrations. Over a two to three hour period samples were collected, at 15 to 30 minute intervals, centrifuged ($6500 \times g$, $2\,min$) and the supernatant isolated. The lactate concentrations of the remaining supernatants of the samples were determined with the NAD^+ and LDH linked enzyme assay. The metabolic flux for each spent culture media sample was calculated using linear regression on the data of lactate concentration vs time.

To measure the quantitative effect of all factors affected by the presences of parasites, spent culture media was collected from the time points of the growth experiments, where the parasites grow through two cycles from rings to schizonts. The supernatants were then incubated with normal uRBCs at 37° C as described above and lactate production rates compared to rates obtained using only pH and/or extracellular lactate as the inhibitors.

Data analyses and model construction All data analyses and simulations were performed using Microsoft Excel and Wolfram Mathematica. The phenomenological model was constructed by fitting mechanism-agnostic exponential functions to the data in Mathematica using the "FindFit"/"NonlinearModelFit" functionality. A mechanistic model that describes the reinvasion event between intra-erythrocytic cycles, the biomass of the parasites and the lactate production by pRBCs and iRBCs in terms of ordinary differential equations, was subsequently constructed. Closed-form solutions for the variables were obtained from the differential equations using function in Mathematica. The model was fitted to experimental data using NMinimize, a function that attempts to minimize the sum of squared differences between the model prediction and experimental data.

Chapter 4

Results and Discussion: Modelling the reinvasion event

4.1 Phenomenological model

4.1.1 Introduction

During the last 14 hours of the parasite's 48 hour intra-erythrocytic phase the DNA content undergoes several rounds of replication. The DNA replication of the parasite is asynchronous, producing 8 to 30 merozoites [9, 47]. These merozoites are released to enter uninfected red blood cells (uRBCs) [62]. Even though the merozoite is very well adapted for invasion, it is widely accepted in literature that the efficiency of reinvasion *in vivo*, termed as the percentage of merozoites that successfully reinvade new RBCs, is rarely over 40% [36]. There is still limited knowledge on the quantification of the reinvasion event which directly influences studies on virulence and drug development.

It is during the intra-erythrocytic phase of the parasite's life cycle that a patient infected with *P. falciparum* will experience pathological symptoms such as lactic acidosis and hypoglycaemia. The exponential growth of the parasite contributes significantly to the decrease in blood glucose and extracellular lactate [11]. The system under investigation consists of uRBCs and parasitized RBCs (pRBCs), both dependent on glycolysis for energy. As glucose is metabolised, lactate is formed and excreted to the extracellular medium. The pRBCs show significant increased metabolic activity, up to a 100 fold that of normal uRBCs, whilst the uRBCs however, show a decrease in metabolic activity in the presence of pRBCs [14, 15]. This increased glycolytic activity significantly contributes to the complications experienced by a patient during the infection mentioned above.

In this section we set out to describe the experimentally determined lactate production of the system with mathematical equations using a phenomenological modelling approach to understand the reinvasion efficiency. This will be done by measuring lactate production of pRBCs over two intra-erythrocytic life cycles experimentally. The experimental data will be fitted with the phenomenological model. The rate of

lactate production just before and after the reinvasion will be used to calculate the loss of active biomass and therefore the reinvasion efficiency.

4.1.2 Results and Discussion

We measured external metabolic products and biomass concentrations over two consecutive life cycles. A *P. falciparum* culture ($\approx 1\%$ Haematocrit and parasitaemia of $\approx 1\%$) prepared with synchronised rings that were about $10h$ post merozoite invasion (pmi). The culture was regularly sampled over an $80h$ period and the lactate concentrations at the time points were determined with $NAD^+ - LDH$ linked enzyme assays.

4.1.2.1 Analysis of experimental results of lactate production

Typical data obtained from growth experiments are shown in Fig 4.1. The incubations include uRBCs and pRBCs, both of which are metabolically active. As a product of glycolysis, the uRBCs produce lactate at a constant rate which lead to a linear increase in external lactate (as the uRBCs are not growing) (simulation results shown in Fig 4.1). The parasites, however, grow within the pRBCs and the biomass increases exponentially, assuming a constant specific growth rate.

Discontinuity in Growth cycles If the lactate production per parasite volume biomass stays constant as found by Du Toit [11], an exponential increase in external lactate would be expected.

In Fig. 4.1(a) the lactate production of both cycles were fitted with a single exponential function (Eq. 4.1.1) to describe the exponential trend. The growth of *P. falciparum* parasites within the blood phase is unique in the fact that at every reinvasion, a fraction of the biomass does not continue into the next cycle leading to a discontinuity observed at the time of reinvasion. As the incubation starts with parasites $10h$ pmi of age, reinvasion, occurs at $38h$ in the experiment (biologically at $48h$ pmi). To describe the lactate production around the point of reinvasion more accurately, two independent exponential functions were applied to each cycle. Fig 4.1 (b) shows two independent exponential fits, where Eq. 4.1.1 and Eq. 4.1.2 were applied to the first and the second cycle respectively

$$f_1(t) = a_1 \cdot e^{\mu_1 \cdot t} \tag{4.1.1}$$

$$f_2(t) = a_2 \cdot e^{\mu_2 \cdot (t - t_R)} \tag{4.1.2}$$

with a_1, a_2 as [lac] at $t = 0h$ and $t = t_R$, μ, μ_2 specific growth rate for the first and second cycle respectively, t represents time in hours, and $t_R = 38h$ reflecting the time off set for the start of the second cycle.

Two independent equations were used to test whether it is possible to describe the data better by fitting the data of each cycle independently (Fig. 4.1 (b)) as opposed

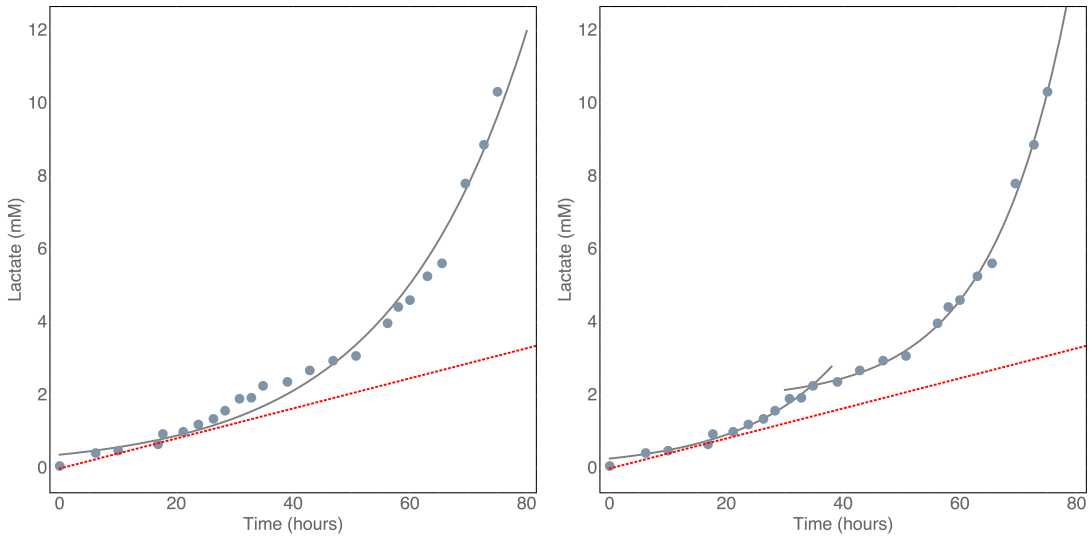

(a) (b)

Figure 4.1: **Lactate production of pRBCs and uRBCs** The experimental data of external lactate measured during an $80h$ pRBC incubation (grey bullets) and the lactate production of uRBCs (red dotted line) simulated over the incubation period from independent uRBC flux measurements. (a) An exponential fit of the total lactate concentrations over both cycles (RSS= 2.701), (b) Independent exponential fits of the total lactate production for each cycle (RSS=0.797).

to a single fit for both cycles (Fig. 4.1 (a)). In Fig 4.1 (a),(b) it can be seen that 2 independent fits describe the data better, specifically the discontinuity observed at the reinvasion time. This is also confirmed by the sums of squared differences between the data and model fit, namely 2.701 for Fig 4.1 (a) and 0.797 for Fig 4.1(b).

The experimental data for lactate production over time are first analysed with a minimal exponential phenomenological model (*analysis I*). Based on the observation that the extracellular lactate concentration increases exponentially over time and displays a discontinuity at the reinvasion time point, a simple phenomenological model of two exponential functions Eq.4.1.1, 4.1.2 is fitted to the data.

However, the data is richer in information than these exponential equations reveal. The experimental data is presented as lactate concentration vs time, and the gradient $\frac{d\text{Lac}}{dt}$ can be related to the specific lactate production rate of the parasite. Du Toit [11] found that the parasitic lactate production per biomass stays constant over the blood-stage life cycle and we can therefore state:

$$\frac{d\text{Lac}}{dt} = k_{Pf} \cdot biomass(t) \tag{4.1.3}$$

where k_{Pf} is the specific lactate production rate constant for *P. falciparum*, biomass(t) represents the total parasite biomass at time t where biomass(t) grows exponentially

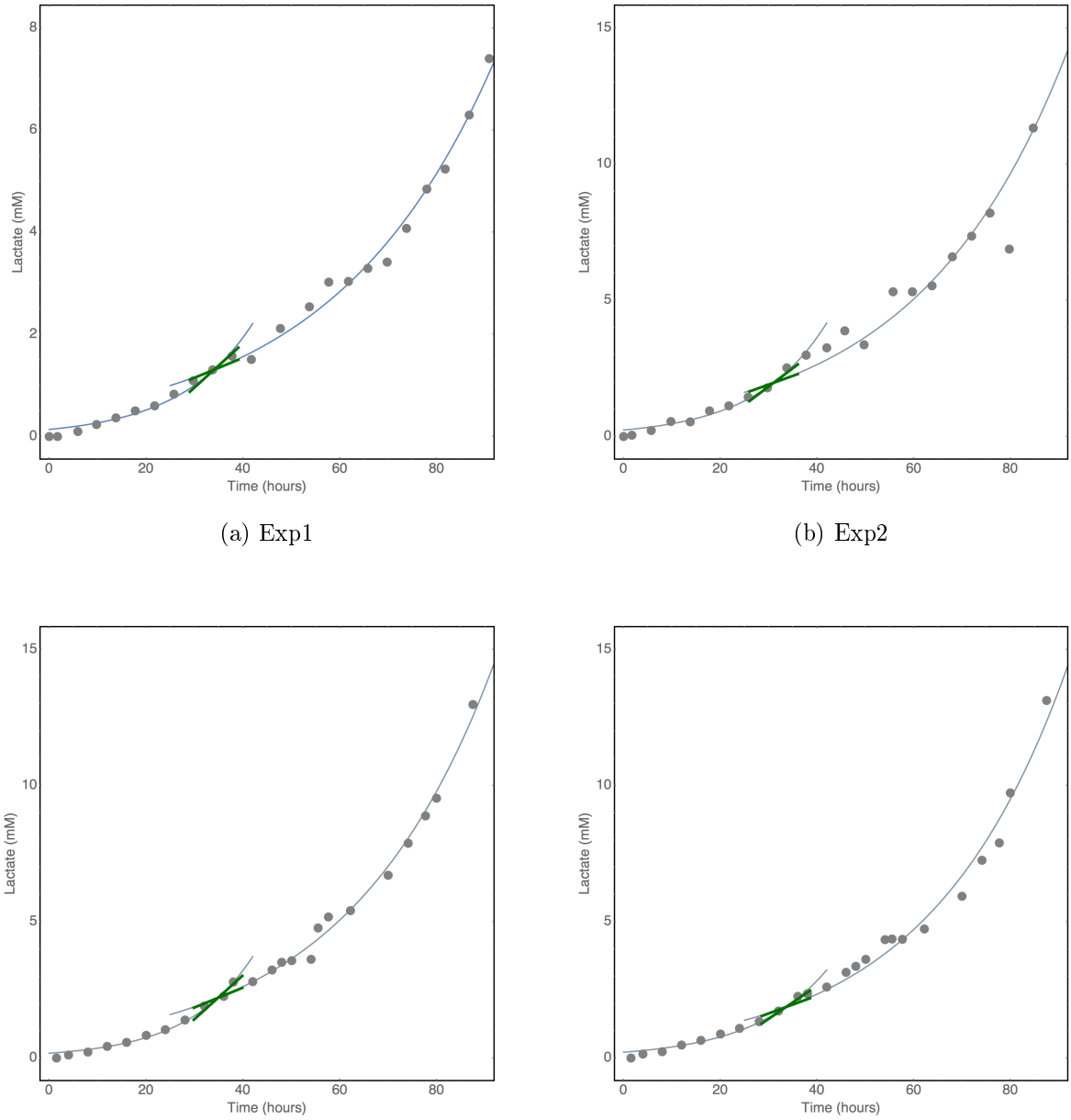

(a) Exp1

(b) Exp2

(c) Exp3

(d) Exp4

Figure 4.2: **A phenomenological model (*analysis I*) fitted over two cycles of *P. falciparum* lactate production.** Experimentally determined lactate production of synchronised *P. falciparum* cultures ($\approx 1\%$ parasitaemia, $\approx 1\%$ Haematocrit) over two consecutive life cycles fitted with simple exponential equations 4.1.1, 4.1.2 (grey line). The rate of lactate production just before and after reinvasion is indicated by the green tangents. The ratio of the two tangents was used to calculate the reinvasion efficiency shown in Table 4.1

over time (starting at time $= 0h$) with a specific growth rate μ :

$$biomass(t) = biomass(0) \cdot e^{\mu_1 t} \qquad \text{for} \quad t < t_R \tag{4.1.4}$$

From literature it is known that not all the merozoites that are released at the end of the first cycle, continue into the next cycle and one would therefore expect a discontinuity at the time of reinvasion [26, 67]. The fraction (< 1) of the produced merozoites successfully continuing into the next cycle is defined as the reinvasion efficiency r. The initial biomass for the second cycle equals $r \cdot biomass(t_R)$ therefore

$$biomass(t) = r \cdot biomass(t_R) \cdot e^{\mu_2 (t - t_R)} \qquad \text{for} \quad t > t_R \tag{4.1.5}$$

where $biomass(t_R)$ is the total parasite biomass just before the reinvasion event.

We can also extend the lactate production rate to describe the lactate production before and after the reinvasion event to

$$\frac{d\mathrm{Lac}_{cycle1}}{dt} = k_{Pf} \cdot biomass(0) \cdot e^{\mu_1 t} \qquad 0 < t < t_R \tag{4.1.6}$$

$$\frac{d\mathrm{Lac}_{cycle2}}{dt} = k_{Pf} \cdot r \cdot biomass(t_R) \cdot e^{\mu_2 (t - t_R)} \qquad t \geq t_R \tag{4.1.7}$$

By substituting Eq 4.1.4 into Eq 4.1.7,

$$\frac{d\mathrm{Lac}_{cycle2}}{dt} = k_{Pf} \cdot r \cdot (biomass(0) \cdot e^{\mu_1 (t_R)}) \cdot e^{\mu_2 (t - t_R)} \qquad t \geq t_R \tag{4.1.8}$$

The ratio between Eq 4.1.6 and Eq 4.1.8 can be seen in Eq 4.1.9

$$\frac{\frac{dLac_{cycle2}}{dt}}{\frac{dLac_{cycle1}}{dt}} = \frac{k_{Pf} \cdot r \cdot (biomass(0) \cdot e^{\mu_1 (t_R)}) \cdot e^{\mu_2 (t - t_R)}}{k_{Pf} \cdot biomass(0) \cdot e^{\mu_1 t}} = r \quad \text{when } \mu_1 = \mu_2 \quad \text{at } t = t_R \tag{4.1.9}$$

Eq 4.1.9 shows that the ratio of the gradients in the lactate production plot for the first and second cycle is equal to the reinvasion efficiency r. Thus, we can estimate r from the discontinuity we observe in the lactate production.

For each of the 9 experiments, the phenomenological model was fitted to the experimental data of which 4 experiments can be seen in Fig 4.2 (the rest of the graphs are

shown in the Appendix, section 6.1). The gradients of the exponential curves immediately before and after the reinvasion, as seen in Fig 4.2, were used to calculate the reinvasion efficiency using Eq 4.1.9. The fitted values for each of the parameters are shown in Table 4.1.

Table 4.1: **Parameter values of phenomenological model (*analysis I*)**. Eq. 4.1.6 and Eq.4.1.8 were fitted to the total lactate production of pRBCs ($\approx$ 1% parasitaemia and $\approx$ 1% Haematocrit) over two consecutive life cycles with the goal of calculating the reinvasion efficiency from the ratio of the gradients where $t = t_R$

Exp	a1 mM	a2 mM	μ_1 (h^{-1})	μ_2 (h^{-1})	r (%)
Exp1	0.138	1.472	0.0660	0.0298	45.23%
Exp2	0.238	2.473	0.0682	0.0324	47.58%
Exp3	0.174	2.451	0.0729	0.0330	45.26%
Exp4	0.212	2.183	0.0649	0.0350	54.00%
Exp5	0.267	4.536	0.0769	0.0299	38.83%
Exp6	0.424	4.025	0.0631	0.0341	53.98%
Exp7	0.696	2.630	0.0375	0.0279	74.37%
Exp8	0.348	6.223	0.0797	0.0287	36.04%
Exp9	0.273	1.821	0.0612	0.0455	74.41%

RBC contribution The majority of RBCs in the experimental incubations are uninfected and also produce lactate from glycolysis. This contributes significantly to the lactate production in the incubation during the early phases of the infection, when the parasites in the pRBCs are still small (just after invasion of a RBC). As the equations described above are pertinent to the lactate production by the parasites only, the contribution by the uRBCs should be subtracted from the total lactate production. Here it is assumed the lactate production rate of uRBCs is given by:

$$\frac{d\text{Lac}_{\text{uRBCs}}}{dt} = k_{\text{uRBCs}} \cdot \text{Number of uRBC} \tag{4.1.10}$$

where k_{uRBC} is the rate constant describing the lactate production for uRBCs.

Taking a closer look at the uRBC's lactate production, we found that the metabolic activity of uRBCs is inhibited (iRBCs) in parasitized cultures as explained in Chapter 2, also shown by Du Toit [11] and Mehta et al. [14, 15]. The mechanism is still unknown but Mehta et al. [14, 15] suggest that the inhibition occurs on the PFK and PK enzymes. Du Toit [11] did preliminary quantification studies on inhibition, and found that the inhibition of uRBC lactate flux in cultures with about $\approx$ 1% parasitaemia amounts to about 22% at $48h$, the end of schizont stage of infection.

Eq. 4.1.10 describes normal lactate production with no inhibition. If a constant inhibition of 22% is assumed, the 78% activity of the RBC flux can be described by multiplying this equation by a factor 0.78 to account for the inhibition.

$$\frac{d\text{Lac}_{\text{iRBCs}}}{dt} = 0.78 \cdot k_{\text{uRBC}} \cdot \text{ Number of uRBC} \tag{4.1.11}$$

Analysis of experimental data To apply Eq. 4.1.9 to the data, we need to correct the total lactate production for the uRBC lactate production, to obtain the rate of lactate production of the pRBCs only.

$$\frac{d[\text{Lac}]_{\text{Total}}}{dt} = \frac{d[\text{Lac}]_{pRBCs}}{dt} + \frac{d[\text{Lac}]_{\text{uRBCs}}}{dt} \tag{4.1.12}$$

$$[\text{Lac}]_{\text{Total}}(t) = [\text{Lac}]_{\text{pRBCs}}(t) + [\text{Lac}]_{\text{uRBCs}}(t) \tag{4.1.13}$$

For each experiment, the uninhibited uRBC flux was experimentally determined, corrected with the assumed inhibition factor (as described above) and subtracted from the total lactate production.

The data analysis is approached in four ways:

- I) with no correction for uRBCs as shown above (Fig 4.2 and Table 4.1),
- II) the total lactate corrected for the contribution of inhibited uRBCS (iRBCs),
- III) total lactate corrected for the contribution of iRBCs with an offset for lactate present at the start of the second cycle,
- IV) total lactate corrected for the contribution of iRBCs with an offset for lactate present at the start of both cycles.

The first analysis (*analysis I*) is shown above in Fig 4.2 and Table 4.1. In Fig.4.3 the phenomenological model (*analysis II* Eq. 4.1.1, 4.1.2) fits are plotted with the experimentally determined lactate concentration, and displayed with the inhibited uRBC lactate production over $96h$. For the second data analysis approach, as mentioned above, the experimental data needs to be corrected by subtracting the contribution of iRBCs from the system. The tangents at reinvasion ($t = 38h$) after correction for the lactate production is equal to the rate of lactate production at the end of the first cycle and the start of the second cycle. The ratio of these two tangents was used to calculate the reinvasion efficiency as shown in Eq. 4.1.9.

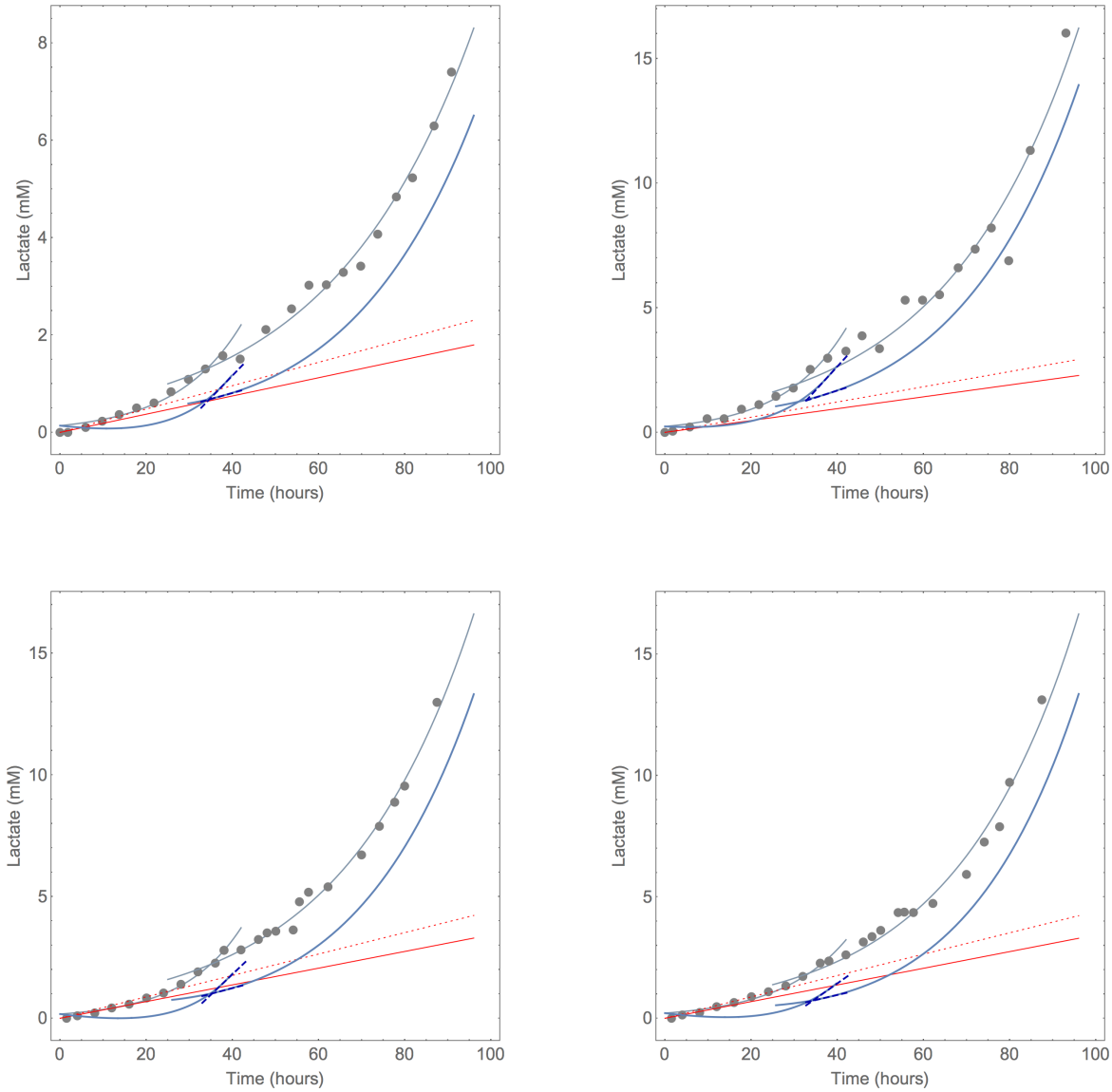

Figure 4.3: **Phenomenological model (*analysis II*) fits to *P. falciparum* lactate production over two life cycles.** Experimentally determined lactate production of synchronised *P. falciparum* cultures ($\approx 1\%$ parasitaemia, $\approx 1\%$ Haematocrit) over two consecutive life cycles fitted with equations 4.1.1, 4.1.2 (grey line), displayed with uRBC lactate production (red dotted) and the inhibited uRBC lactate production simulated with Eq.4.1.11 (solid red) .The solid blue lines represent the corrected lactate production for pRBCs, iRBCs. The two tangents at the point of reinvasion indicate the rate of lactate production by pRBCs at the end of the first cycle and the start of the second cycle.

The results of the parameters fitted during *analysis II* with the corrected lactate production for pRBCs for 9 experiments are shown in Table 4.2.

Table 4.2: **Parameter values of phenomenological model (*analysis II*)** fitted to the total lactate production of pRBCs ($\approx 1\%$ parasitaemia and 1% Haematocrit) over two consecutive life cycles

Exp	a1 (mM)	a2 (mM)	μ_{s1} (h^{-1})	μ_{s2} (h^{-1})	r (%)
Exp1	0.138	1.472	0.0660	0.0298	27.19%
Exp2	0.238	2.473	0.0682	0.0324	29.52%
Exp3	0.174	2.451	0.0729	0.0330	27.66%
Exp4	0.212	2.183	0.0649	0.0350	33.22%
Exp5	0.267	4.536	0.0769	0.0299	31.17%
Exp6	0.424	4.025	0.0631	0.0341	34.41%
Exp7	0.696	2.630	0.0375	0.0279	39.71%
Exp8	0.348	6.223	0.0797	0.0287	29.42%
Exp9	0.273	1.821	0.0612	0.0455	27.79%

The ratio of the rate of lactate production (Eq.4.1.9) was used to calculate the reinvasion efficiency with the average reinvasion efficiency calculated for 9 experiments as $31.7\% \pm 4.2\%$ during *analysis II*. Although these initial results seem to show correlation with values found in literature such as the reinvasion efficiency of 25% by Reilly et al. [10], the phenomenological model fits in *analysis II* shown in Fig.4.3, lactate produced at the point of reinvasion is underestimated by the model compared to the experimental data. Correct description of the lactate around the point of reinvasion is necessary as we use this point to calculate the reinvasion efficiency from the ratio of the tangents.

Although the lactate is used to represent the growing biomass as explained in Eq. 4.1.4, 4.1.7, lactate can be present in the culture when the experiment starts or after the first reinvasion that does not represent the growing biomass. To account for this the phenomenological model was adjusted to include an offset c_2 in the exponential function of the second cycle in *analysis III*:

$$f_1(t) = a_1 \cdot e^{\mu_1 \cdot t} \tag{4.1.14}$$

$$f_2(t) = a_2 \cdot e^{\mu_2 \cdot (t - t_R)} + c_2 \tag{4.1.15}$$

where c_2 is the external $[lac]$, that does not represent the active biomass at $t = t_R$.

The experimental data was refitted with the adjusted phenomenological model in *analysis III* and the fits are shown in Fig. 4.4.

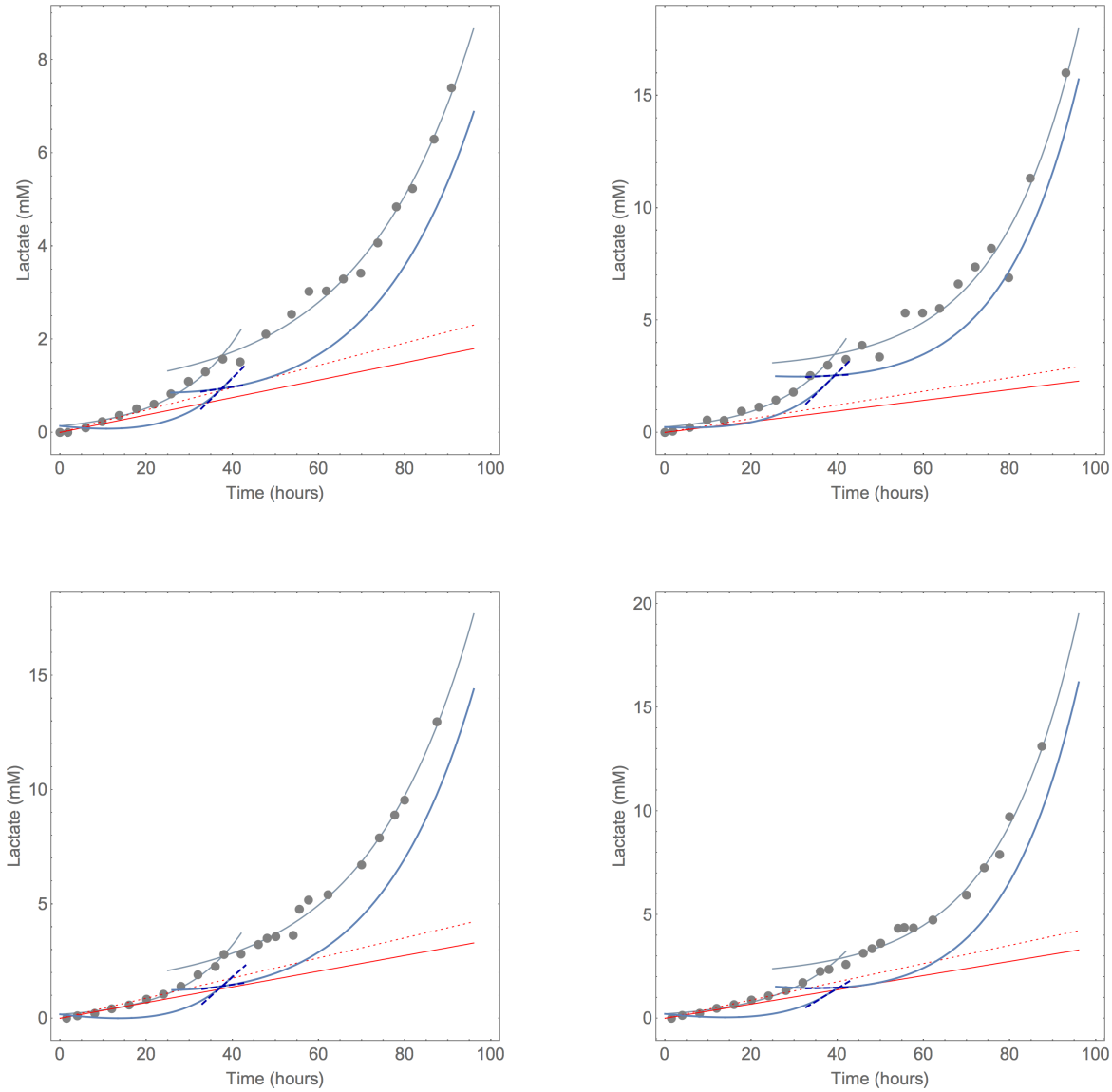

Figure 4.4: **Phenomenological model (*analysis III*) fits to *P. falciparum* lactate production over two life cycles.** Experimentally determined lactate production of synchronised *P. falciparum* cultures ($\approx 1\%$ parasitaemia, $\approx 1\%$ Haematocrit) (grey dotted) over two consecutive life cycles fitted with equations Eq.4.1.14 and 4.1.15 (grey lines), displayed with uRBC lactate production (red dotted) and the inhibited uRBC lactate production simulated with Eq.4.1.11 (solid red). The solid blue lines represent the corrected lactate production for pRBCs. The two dark blue tangents at the point of reinvasion indicate the rate of lactate production by pRBCs at the end of the first cycle and the start of the second cycle.

From the graphs (Fig 4.4) it is evident that the rates of lactate production at the time of reinvasion after correction for inhibition, result in negative rates for some of

the experiments (see the second cycle in Fig 4.4 (b, d)). These rates are not realistic, since negative lactate productions rates (i.e lactate consumption) are unlikely.

Table 4.3: **Parameter values of phenomenological model (*analysis III*)** fitted to two life cycles of *P. falciparum* lactate production and calculated reinvasion efficiency.

Exp	$a_1\ (mM)$	$a_2\ (mM)$	$\mu_1\ (h^{-1})$	$\mu_2\ (h^{-1})$	$c_2\ (mM)$	$r(\%)$
Exp1	0.138	0.868	0.0660	0.0381	0.79	15.30%
Exp2	0.238	0.635	0.0682	0.0548	2.79	5.57%
Exp3	0.174	1.519	0.0729	0.0411	1.20	16.72%
Exp4	0.212	0.744	0.0649	0.0544	2.03	4.48%
Exp5	0.267	3.648	0.0769	0.0331	1.14	26.95%
Exp6	0.424	0.973	0.0631	0.0613	4.22	4.44%
Exp7	0.696	0.332	0.0375	0.0746	2.79	-45.59%
Exp8	0.348	7.678	0.0797	0.0250	-1.52	32.84%
Exp9	0.273	0.526	0.0612	0.0751	1.87	-14.25%

For completeness the phenomenological model was adjusted again (*analysis IV*) to include an offset c_1 in the exponential function of the first cycle, to account for possible lactate present at the start of the first cycle that does not represent the growing biomass as described in Eq. 4.1.7 :

$$f_1(t) = a \cdot e^{\mu_1 \cdot t} + c_1 \tag{4.1.16}$$

$$f_2(t) = a_2 \cdot e^{\mu_2 \cdot (t - t_R)} + c_2 \tag{4.1.17}$$

The fits were repeated with the phenomenological model in *analysis IV* and the results shown in Table 4.4.

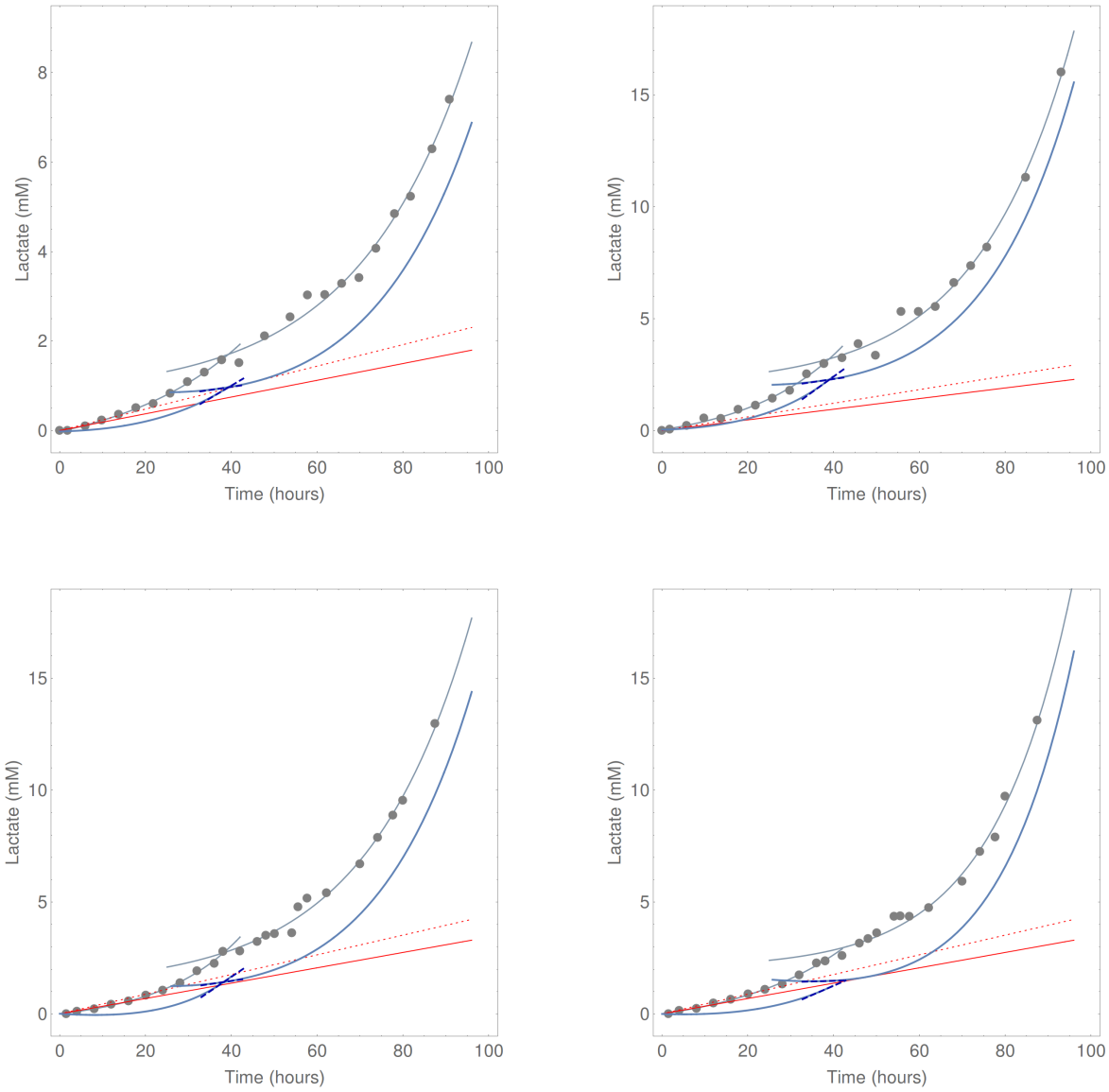

Figure 4.5: **Phenomenological model (*analysis IV*) fits to *P. falciparum* lactate production over two life cycles.** Experimentally determined lactate production of synchronised *P. falciparum* cultures ($\approx 1\%$ parasitaemia, $\approx 1\%$ Haematocrit) (grey dotted) over two consecutive life cycles fitted with equations Eq.4.1.16 (grey lines), displayed with uRBC lactate production (red dotted) and the inhibited uRBC lactate production simulated with Eq.4.1.11 (solid red) .The solid blue lines represent the corrected lactate production for pRBCs. The two dark blue tangents at the point of reinvasion indicate the rate of lactate production by pRBCs at the end of the first cycle and the start of the second cycle.

Table 4.4: **Parameter values of phenomenological model (*analysis IV*)** fitted to two life cycles of *P. falciparum* lactate production and calculated reinvasion efficiency.

Exp	a_1 (mM)	a_2 (mM)	$\mu_1(h^{-1})$	$\mu_2(h^{-1})$	c_1 (mM)	c_2 (mM)	r (%)
Exp1	0.611	0.868	0.0341	0.0381	-0.63	0.79	24.62%
Exp2	0.675	0.635	0.0447	0.0548	-0.64	2.79	7.58%
Exp2	0.675	1.166	0.0447	0.0450	-0.64	1.99	20.24%
Exp3	0.421	1.519	0.0527	0.0411	-0.42	1.20	21.65%
Exp4	0.758	0.744	0.0376	0.0544	-0.76	2.03	6.72%
Exp5	0.912	3.648	0.0488	0.0331	-1.07	1.14	36.94%
Exp6	0.427	0.973	0.0630	0.0613	-0.01	4.22	4.45%
Exp7	11.944	0.332	0.0048	0.0746	-11.54	2.79	-142.06%
Exp8	1.182	7.678	0.0501	0.0250	-1.32	-1.52	45.07%
Exp9	0.599	0.526	0.0432	0.0751	-0.46	1.87	-19.17%

In *analysis IV* in Fig.4.5, the model represents the experimental data more closely, especially the lactate around time of reinvasion $t = 38h$ is described better, which was a challenge earlier. The interpretation the fits however reveals a negative [lac] at $t = 0h$, which is not biologically possible and leads to very high specific growth rates. The reinvasion efficiencies calculated in this analysis is biologically possible but includes big variance which will be further discussed when calculating the merozoites below.

Merozoite Calculation The reinvasion efficiency r is defined as the fraction of merozoites (or parasitic biomass) that successfully continues to grow after the reinvasion process. The reinvasion efficiency and the average merozoites produced per schizont can therefore described as

$$r = \frac{\text{Par}_{cycle2} \cdot \text{Cellcount}_{uRBCs}}{\text{Par}_{cycle1} \cdot \text{Cellcount}_{uRBCs} \cdot m} \tag{4.1.18}$$

$$m = \frac{\text{Par}_{cycle2} \cdot \text{Cellcount}_{uRBCs}}{\text{Par}_{cycle1} \cdot \text{Cellcount}_{uRBCs} \cdot r} \tag{4.1.19}$$

where r represents the reinvasion efficiency, Par the parasitaemia in the cycle mentioned, m the average merozoites release by a schizont.

The microscopically determined parasitaemia and RBC counts, together with the r value, estimated from the tangent of the iRBC lactate production plots, were used to calculate the number of merozoites that had to be released to amount to the parasitaemia in the second cycle using Eq. 4.1.19. Results for each experiment are shown in Table 4.5.

Table 4.5: **Merozoite calculations** The reinvasion determined by each of the phenomenological model analyses (I-IV) was used to calculate the number of merozoites released for each experiment using the microscopically determined percentage parasitaemias

Exp	Par_{cycle1}	Par_{cycle2}	I		II		III		IV	
			r	m	r	m	r	m	r	m
Exp1	0.86%	6.00%	45.23%	15	27.19%	26	15.30%	45	24.62%	28
Exp2	2.00%	11.00%	47.58%	11	29.52%	18	5.57%	97	20.24%	27
Exp3	1.07%	8.03%	45.26%	16	27.66%	27	16.72%	44	21.65%	34
Exp4	1.07%	8.03%	54.00%	14	33.22%	22	4.48%	166	6.72%	110
Exp5	2.63%	11.00%	38.83%	11	31.17%	13	26.95%	15	36.94%	11
Exp6	1.65%	6.20%	53.98%	7	34.41%	11	4.44%	83	4.45%	83
Exp7	1.15%	2.84%	74.37%	3	39.71%	6	-45.59%	-5	-142.06%	-2
Exp8	2.15%	10.78%	36.04%	14	29.42%	17	32.84%	15	45.07%	11
Exp9	1.29%	5.43%	74.41%	6	27.79%	15	-14.25%	-29	-19.17%	-22

Analysis I of the phenomenological model described the lactate production of the incubations quite well and led to reinvasion efficiencies of between 36.04% to 74.4% and 3 to 16 merozoites with an average of 10.7. As the phenomenological models plot two complete independent functions on each cycle, a prediction of the time of reinvasion can be obtained from the intersection of the two exponential functions. *Analysis II* seemed to predict the reinvasion point earlier than the biological time of reinvasion, $38h$ ($48h$ *pmi*). After the lactate contribution of uRBCs was subtracted, the rate of pRBCs lactate production just before and after reinvasion led to reinvasion efficiency results between 27.19% to 39.71% and 6 to 27 merozoites with an average of 17.2. For *analysis III* of the phenomenological model an offset was included to account for the lactate present at the start of the second cycle. The model fit improved around the reinvasion event but when the lactate contribution of uRBCs was subtracted we noticed in some of the experiments eg. Fig 4.4 (d) that the rate of lactate production at the start of the second cycle becomes negative which would imply the consumption of lactate, which is biologically unlikely. The negative lactate production could be due to an overestimation of the lactate contributed by the uRBCs, which skews the gradients around the reinvasion event. This resulted in a very big range in both the reinvasion efficiency of $-45,59\%$ to 32.84% and the merozoites of -5 to 166 with average of 47.9. In the fourth analysis phenomenological model (*analysis IV*) offsets for both cycles were included and resulted in a reinvasion efficiency between -142% to 36% that lead to the number of merozoites varying between $-2-110$ with average of 31.11.

As the reinvasion efficiency is dependent on various factors it is understandable that it varies between experiments, the average number of merozoites however, is expected to stay constant between biological repeats for a specific *Plasmodium* strain if it is an inherent characteristic of the strain due to regulatory checkpoints present as mentioned in Chapter 2. The phenomenological model was able to describe the data sets quite well, but the analysis of the fitted parameters led to unrealistic results for some of the experiments. The negative reinvasion efficiencies of experiment 7, for example lead to merozoite numbers ranging between -5 and 165.6. We therefore choose to use a more mechanistic approach to analyse the data.

The incorporation of the constant inhibition of 22% in this model it is a strong simplification that is not necessarily realistic. We have tried to correct the uRBC lactate production which lead to completely unrealistic results.

4.2 Constructing a mechanistic reinvasion model

4.2.1 Introduction

Detailed mathematical models for glucose metabolism of *Plasmodium falciparum* within its host red blood cell (RBC) were constructed by Penkler [16] and Du Toit [11]. These models predict lactate production during one life cycle (48 hours) of the parasite with reasonable accuracy. Extension over multiple life cycles requires quantitative information about the reinvasion process between life cycles, such as the number of merozoites released on erythrocyte lysis and efficiency of reinvasion into new red blood cells (RBCs) [11]. Our current mathematical models do not include a quantitative description of this reinvasion process.

In Section 4.1 a simple phenomenological model with exponential equations was fitted to lactate concentrations measured over two 48 hour-cycles of parasitic growth. The reinvasion efficiency of the parasites was determined from the fits and this enabled us to calculate the average number of merozoites produced. For some of the experiments this resulted in unrealistic values for reinvasion efficiency and the number of merozoites produced.

In this section, we set out to construct a more mechanistic kinetic model that describes the lactate production over two consecutive intra-erythrocytic life cycles of *P. falciparum*, growing in human erythrocytes. The model includes the lactate production by uRBCs and pRBCs and is tested in its ability to predict the lactate production during growth experiments. The model is then fitted to experimental data to gain more quantitative insight into the reinvasion process.

4.2.2 Model construction

The system consists of lactate producing RBCs of which 1-8% are infected with *P. falciparum*. Strictly speaking the lactate produced by the pRBC is the sum of the lactate produced by the parasite inside the pRBC and the RBC's own activity. Since the lactate production rate of the host RBC is much smaller than the parasites inhabiting it, its contribution will be ignored in the case of pRBCs. Although the flux of the uRBCs is about 40 times less than that of pRBCs, only 1-8% of the RBCs are infected with *P. falciparum*. Therefore the uRBCs still significantly contribute to the total lactate produced, particularly when the parasites in the pRBCs are still in ring and young trophozoite phase. At any time (t) the total lactate in the system is the sum of lactate produced by uninfected RBCs (uRBCs) and parasitized RBCs (pRBCs) given by:

$$[\text{Lac}]_{\text{Total}}(t) = [\text{Lac}]_{Pf}(t) + [\text{Lac}]_{\text{uRBCs}}(t) \tag{4.2.1}$$

and the rate of lactate production by the system is the sum of the lactate production by the uRBCs and the pRBCs:

$$\frac{d[\text{Lac}]_{\text{Total}}}{dt} = \frac{d[\text{Lac}]_{Pf}}{dt} + \frac{d[\text{Lac}]_{\text{uRBCs}}}{dt} \tag{4.2.2}$$

Lactate production by *Plasmodium falciparum* Du Toit [11] showed that the rate of lactate production of a pRBC, stays constant per parasite biomass volume and therefore increases proportionally as the parasite grows. We can therefore assume that

$$\frac{d\text{Lac}_{Pf}}{dt} = k_{Pf} \cdot biomass(t) \tag{4.2.3}$$

where k_{Pf} is the specific lactate production rate for *P. falciparum* and $biomass(t)$ refers to the parasite biomass.

As shown by Du Toit [11], the biomass of a parasite will increase exponentially over time with a specific growth rate μ and can be described by:

$$biomass(t) = biomass(0)e^{\mu t}. \tag{4.2.4}$$

The rate of lactate production of pRBCs can be described by combining Eq. 4.2.3 and Eq. 4.2.4:

$$\frac{d[\text{Lac}]_{Pf}}{dt} = k_{Pf} \cdot biomass(0)e^{\mu t}. \tag{4.2.5}$$

Lactate production by uRBCs The other component in our system, the non-growing uRBCs, normally produce lactate at a constant rate per uRBC and can therefore be described using:

$$\frac{d[\text{Lac}]_{\text{uRBCs}}}{dt} = k_{\text{uRBCs}} \cdot \text{Number of RBC}, \tag{4.2.6}$$

where k_{uRBC} is a specific lactate production rate constant for uRBCs and since the RBCs do not grow, there is no need to include a growth factor.

Inhibition of uRBCs due to pH and [lactate] In this study we found (as Du Toit [11] and Mehta et. al [14, 15] did) that the uRBCs within the environment of growing parasites show a decrease in the glycolytic flux, (refer to Chapter 2). The parasitic metabolic activity has three effects on the environment: 1) an increase in external lactate, 2) a decrease in pH, and 3) an inhibition of uRBCs' metabolic activity which has been introduced in the previous section. In this section we further

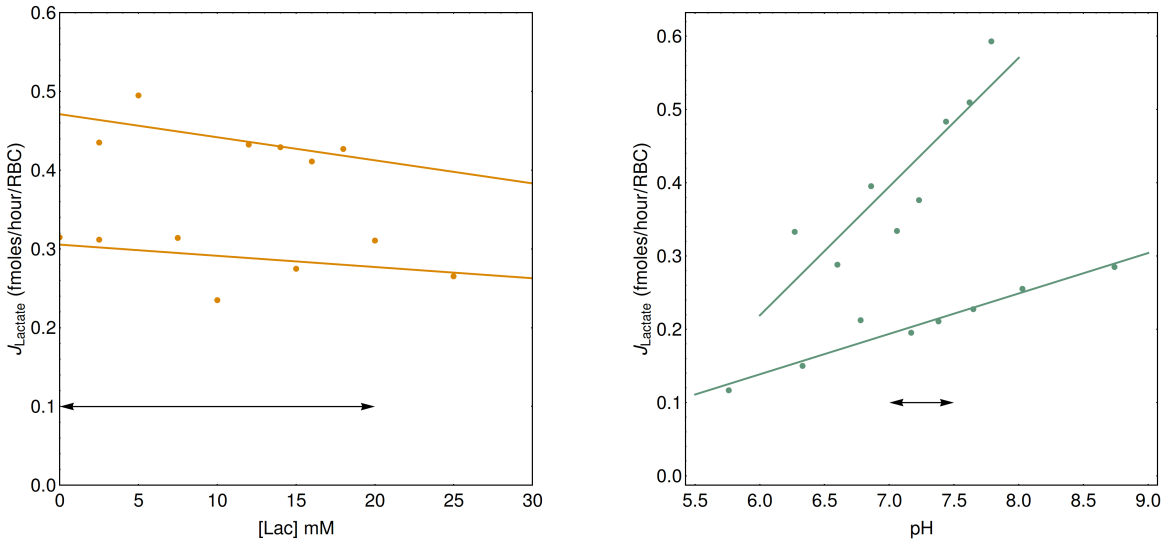

(a) External lactate

(b) pH

Figure 4.6: **Inhibition of uRBC lactate production by pH and lactate concentrations.** Lactate production as a function of externally added lactate, and medium pH, is shown in figures (a) and (b) respectively. The experiments were performed in two independent cultures and the line shows the linear regression for the data points. Physiological ranges, the ranges of [lac] and pH variance within our experiments for both entities are indicated in the graphs by the double-sided arrows.

quantify the effect of pH, extracellular lactate and parasite inhibition on the uRBCs metabolic activity.

The results shown in Fig.4.6 confirm that a decrease in pH and increase in external lactate concentration, do indeed have an inhibitory effect on the uRBC's metabolic activity. The black arrow in Fig 4.6(a) shows the typical range of external lactate concentration within the incubation experiments which range between $0 - 20\,mM$. Between these boundary lactate concentrations the metabolic flux decrease from $0.471 - 0.412\,mM$ and $0.306 - 0.277\,mM$. The average decrease in metabolic flux due to a change in external lactate could maximally amount to 10.8%. The typical pH ranges within the incubation experiments is $7.0 - 7.5$ shown by the black arrow in Fig.4.6 (b). This change in pH led to a difference in metabolic flux of $0.483 - 0.394\,mM$ and $0.22 - 0.194\,mM$. The average decrease in metabolic flux due to a change in pH could maximally amount to 15.33%. Fig.4.6 thus shows the result of 1) an increase in external lactate and 2) a decrease in pH independently on the metabolic flux of uRBCs.

During the incubation at each sample point the pH and lactate concentrations was determined. The extent of expected inhibition due to a change in pH and lactate concentration within the parasitic growth cycles was calculated by using the linear

regression curves in Fig.4.6 and the measured progression values of pH and lactate in a parasitized RBC culture. Thus we assume that the inhibitory effect of lactate and pH is additive

The total inhibition was measured by incubating uRBCs in spent media samples from a parasitized RBC culture obtained at different time points in the parasitic growth cycle. The uRBC flux was determined at each time point and the ratio of $\frac{J_{iRBCs}}{J_{uRBCs}}$ was determined.

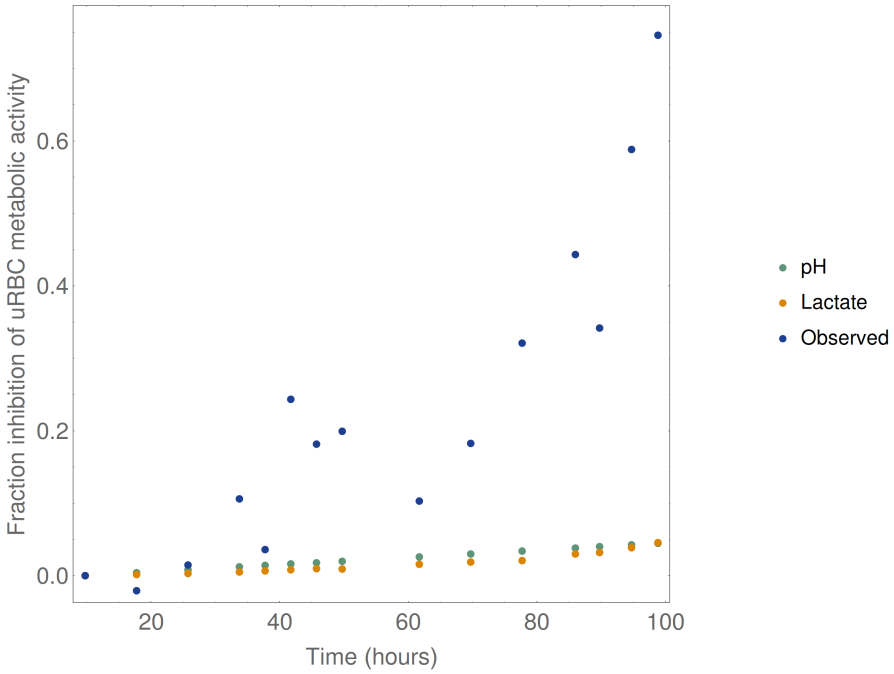

Figure 4.7: **The fraction inhibition on uRBC in a parasitized culture** The hypothetical fraction inhibition on uRBC by the pH (green), lactate concentrations(yellow) compared to the actual inhibition measured during an uRBC incubation with spent media from pRBC(blue) as a percentage of uRBC lactate flux

At every sample point during the 96h growth experiment the [lactate] and pH were measured experimentally. The expected inhibition, based on pH and [lactate] inhibition studies were calculated and are displayed with the actual observed inhibition in Fig 4.7. At around 95h the uRBCs experience 58.8% inhibition where as the pH and external lactate can contribute only to 4.3% and 3.9% each respectively. Assuming that the inhibition of pH and external lactate is additive, the total of 8.2% inhibition reveals that the changes in [lactate] and pH in the media do not account for the actual inhibition experienced by the uRBCs in the incubations.

The degree of actual inhibition increased exponentially over time in the incubation. We therefore agree with Mehta et al. [14, 15] that another independent inhibitor or

inhibitory effect is at play which remains unknown. Although we do not know the nature of the inhibitor, we might still be able to include the inhibitory effect in our model.

Inhibition mechanism Since we have no knowledge of the inhibitor itself, we cannot measure its concentration or estimate the binding constant (K_i) of the inhibitor. Experimentally we can measure the extent that the uRBCs are inhibited by plasmodial activity as an inhibition factor, (i.e. $\frac{J_{iRBCs}}{J_{uRBCs}}$). The results of the inhibition studies have shown similarities to the results in the growth experiment i.e. the exponential trend and the discontinuity at the time of reinvasion.

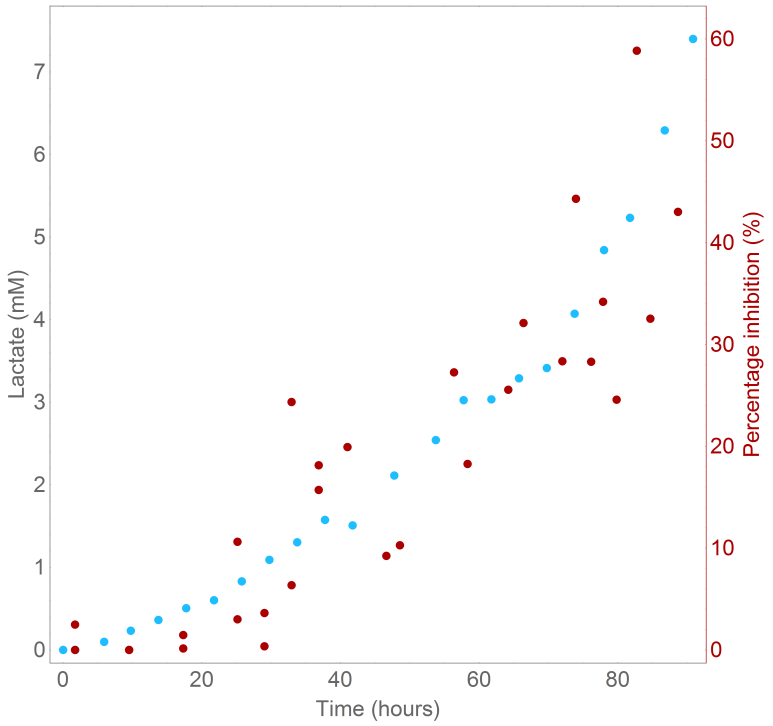

Figure 4.8: **Lactate as a proxy for inhibition** The total lactate produced by *P. falciparum* (blue) and the percentage inhibition (red) experienced by uRBC within an environment of growing parasites over two cycles. Spent media from ≈ 1% *P. falciparum* pRBCs incubation of ≈ 1% Hematocrit sampled at regular time intervals, was incubated with normal uRBc to determine the inhibition of uRBC over the two life cycles

This indicated that the [inhibitor] possibly increased as a product of parasitic growth. Since lactate is also produced as a product of parasitic growth, we used [lactate] as a proxy for the inhibitor (Fig 4.8).

$$[I](t) = k_i \cdot [Lac(t)] \tag{4.2.7}$$

$$\frac{d[I]}{dt} = k_i \cdot k_{Pf} \cdot biomass(t) = k_i \cdot k_{Pf} \cdot biomass(0) \cdot e^{\mu t} \tag{4.2.8}$$

$$I(t) = \frac{k_i \cdot k_{Pf}}{u} \cdot biomass(0) \cdot (e^{\mu t} - 1) \tag{4.2.9}$$

We analysed the inhibitory effect as a function of $\frac{[Lac](t)}{K_i'}$, where the Ki' incorporates the proportionality constant k_i and the binding constant K_i for the inhibition ($K_i' = \frac{Ki}{k_i}$). We used a simple inhibitory mechanism to simulate the inhibitory effect:

$$J_{iRBCs} = J_{uRBCs} \cdot \frac{1}{1 + \frac{[I]}{K_i}} = J_{uRBCs} \cdot \frac{1}{1 + \frac{[Lac(t)]}{K_i'}}. \tag{4.2.10}$$

Equation 4.2.10 describes the lactate production rate by the inhibited uninfected RBCs (iRBCs), including the inhibition by *P. falciparum*, using lactate as a proxy for the real inhibitor.

It is now possible to describe the lactate from the iRBCs in the presence of pRBCs in culture.

4.2.2.1 Constructing the reinvasion model

The parasites grow exponentially from merozoites to schizonts over 48 hours as described by Eq. 4.2.4. At $t = 48h$ the RBC bursts open to release the new merozoites. Not all of the merozoites reinvade successfully into new RBCs and those that do not, die shortly thereafter. This leads to a decrease in biomass at each reinvasion point. The biomass over the first $96h$ is therefore given by:

$$biomass(t) = \left\{ \begin{array}{cc} biomass(0) \cdot e^{\mu t} & t < t_R \\ r \cdot biomass(t_R) \cdot e^{\mu_2 (t - tR)} & t \geq t_R. \end{array} \right\} \tag{4.2.11}$$

Here we allow for a different specific growth rate in the second growth cycle to permit any additional effects on growth not currently reflected explicitly in the formulation. As the lactate produced by the parasite is dependent on the active/growing biomass (Eq.4.2.11), the lactate production rates expands to Eq.4.2.12 and 4.2.13 for the parasite or pRBC and the iRBC respectively, to describe lactate production during the $48h$ before and after the $48h$ reinvasion event :

$$\frac{dLac_{Pf}}{dt} = \left\{ \begin{array}{cc} k_{Pf} \cdot biomass(0) \cdot e^{\mu t} & t < t_R \\ k_{Pf} \cdot r \cdot biomass(t_R) \cdot e^{\mu_2 (t - t_R)} & t \geq t_R \end{array} \right\} \tag{4.2.12}$$

$$\frac{dLac_{\text{iRBCs}}}{dt} = \left\{ \begin{array}{cc} \dfrac{dLac_{\text{uRBCs}}}{dt} \cdot \dfrac{1}{1 + \dfrac{\dfrac{k_{Pf}}{\mu} \cdot biomass(0) \cdot (e^{\mu t} - 1)}{Ki'}} & t < t_R \\ \dfrac{dLac_{\text{uRBCs}}}{dt} \cdot \dfrac{1}{\dfrac{\mathrm{c1}_{r\mu e^{t_R \mu} \left(e^{\mu_2 (t - t_R)} - 1\right)}}{\mu_2} + \mathrm{c1}\left(e^{t_R \mu} - 1\right) + 1} & t \geq t_R \end{array} \right\} \tag{4.2.13}$$

with $c1 = \frac{k_{Pf} biomass(0)}{Ki \mu_1}$, where k_{Pf} is the constant that describes the rate of lactate production ($\mu moles\, h^{-1}$) per parasite volume (μl)).

Eq.4.2.12 and 4.2.13 were integrated with respect to time to get Eq.4.2.14 and 4.2.15 that describes the concentration of lactate as a function of time t.

$$Lac_{Pf}(t) = \left\{ \begin{array}{cc} \frac{k_{Pf}}{\mu} \cdot biomass(0) \cdot (e^{\mu t} - 1) & t < t_R \\ \frac{k_{Pf}}{\mu \cdot \mu_2} \cdot biomass(0) \cdot e^{t_R \mu} \left(r\mu \left(e^{(\mu_2)(t - t_R)} - 1\right) + \mu_2\right) - \mu_2 & t \geq t_R \end{array} \right\} \tag{4.2.14}$$

$Lac_{iRBC}(t) =$

$$\left\{ \begin{array}{cc} \mathrm{k}_{\text{uRBCs}} \frac{\left(\log\left(\mathrm{c1}\left(e^{t\mu_1} - 1\right) + 1\right) - t\mu_1\right)}{(\mathrm{c1} - 1)\mu} & t < t_R \\ \mathrm{k}_{\text{uRBCs}} \left(\frac{\log\left(\mathrm{c1}\left(e^{(\mu_1 t_R)}\left(r\mu_1\left(e^{(\mu_2 (t - t_R))} - 1\right) + \mu_2\right) - \mu_2\right) + \mu_2\right) - \log\left(\mu_2\left(\mathrm{c1}\left(e^{(\mu t_R)} - 1\right) + 1\right)\right) + \mu_2 (t_R - t)}{\mathrm{c1} e^{(\mu t_R)}(r\mu - \mu_2) + (\mathrm{c1} - 1)\mu_2} \right) & t > t_R \\ + \left(\frac{\log\left(\mathrm{c1}\left(e^{(\mu t_R)} - 1\right) + 1\right) - t_R \mu}{(\mathrm{c1} - 1)u} \right) & \end{array} \right\} \tag{4.2.15}$$

and total lactate in the system is sum of fluxes from pRBCs and iRBCs, Eq.4.2.14 and 4.2.15:

$$Lac_{tot}(t) = Lac_{Pf} + Lac_{iRBC} \tag{4.2.16}$$

4.2.2.2 Initial model test

To test the proposed model we used experimentally determined parameter values (Table 4.6) [11], a growth rate factor within the range mentioned by Du Toit and a literature value of 30% for the reinvasion efficiency [29]. Three combinations of parameter sets were tested:

1. a constant specific growth rate over both cycles, and 100% reinvasion,
2. a constant growth rate over both cycles with reinvasion efficiency of 30% and
3. a decrease of 99% growth rate from the first cycle to the second cycle with a 100% reinvasion.

The first and third combination served as a validation that the existence of the discontinuity could not be attributed to a slower growth rate in the second cycle. As seen in Fig 4.9, the model with experimental and literature parameter values (See Table 4.6) can describe the data fairly well, therefore we decided to use our complete data sets to fit the reinvasion efficiency.

Table 4.6: **Parameters for model test**

Pars	Description	Value	Units
K_i	Apparent inhibition constant	10	mM
k_{Pf}	Parasitic specific lactate production rate	0.9	$\frac{\mu moles\ Lac}{\mu L\ parasitic\ biomass} \cdot h^{-1}$
k_{uRBC}	uRBC specific lactate production rate	0.253×10^{-3}	$\frac{\mu moles}{fL_{\mathrm{RBC}}} \cdot h^{-1}$
RBCs	Number of RBC in an Incubation		
t_R	time of reinvasion event	48	hours
μ	Specific growth rate of cycle 1	0.066	h^{-1}
μ_2	Specific growth rate of cycle 2	0.066	h^{-1}
x0	Parasitic biomass at $t = 0h$	1.03×10^8	fL/ml incubation

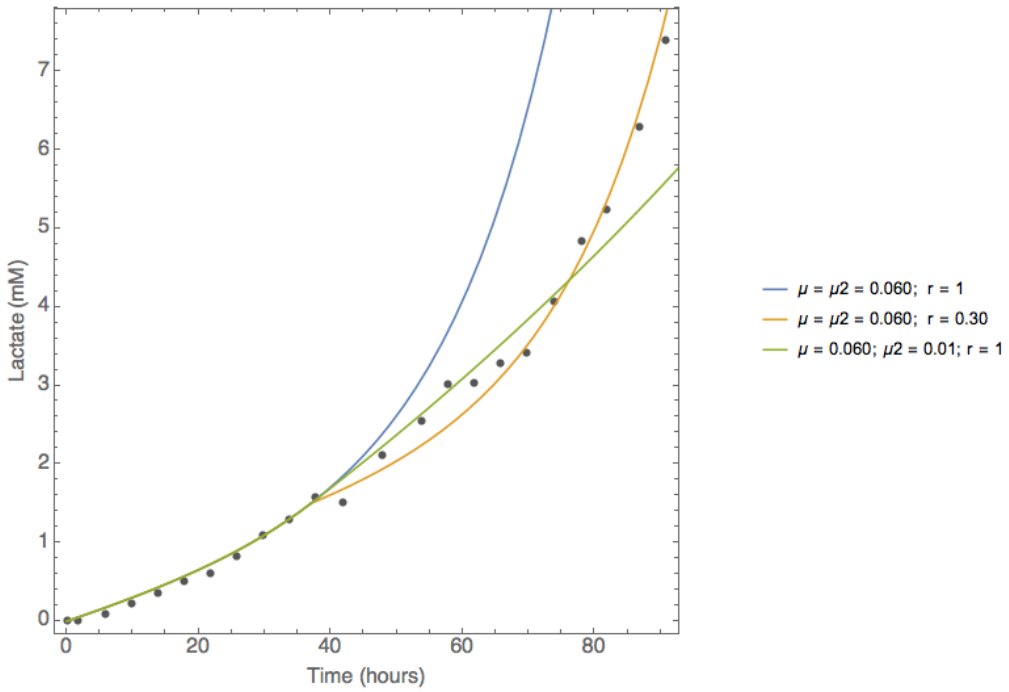

Figure 4.9: **Mechanistic model tested with experimental data** The blue curve indicates a constant specific growth rate over both cycles with a 100% reinvasion efficiency. The green curve indicates a 100% reinvasion efficiency with a dramatic decrease in the growth rate in the second cycle. The orange curve indicates a constant growth rate and a reinvasion efficiency of 30%

4.2.3 Analysis

Brief overview of analysis protocol After the model was constructed and tested with independently determined fitted parameters, it was used to fit to the experimental lactate produced during two life cycles to obtain new values for some of the parameters. Model fitting was conducted by minimizing the sum-of-squared-differences using the "NMinimize" function in Wolfram Mathematica. The combination of parameters to be fitted was selected based on identifiability studies. Three fitting procedures were used. First we assume that biologically the specific growth rate should stay constant and therefore we A) constrain μ to be equal to μ_2 with fixed t_R. The phenomenological model fits however, showed a decrease in the specific growth rate in the second cycle. To account for possible changes in the specific growth rate we also fit for B) independent μ values for respective cycles. Due to asynchronicity of parasites at start of the experiment and variation between experiments the parameter for C) the time of reinvasion t_R was also included to (B) for the third fit.

Identifiability of parameters Re-parameterization was conducted for all the parameters not determined experimentally i.e the specific growth rate for each cycle μ, μ_2, the apparent inhibition constant Ki' and reinvasion efficiency r. The time of

reinvasion (t_R) is not necessarily equal for all cells due to a degree of asynchrony in the life cycle. To estimate the range of t_R, the time points where reinvasion started and ended were observed microscopically (as the time when extracellular merozoites appear and the time when no extracellular merozoites remained). In the model the reinvasion time point is a single value which should be interpreted as an average reinvasion time (t_R) parameter. Values of t_R were also included in the fitting procedure and constrained by the experimentally observed range of t_R values during the growth experiment. The values for the specific growth rate for each cycle μ, μ_2 were found in literature but they varied considerably and were therefore included in the fitting procedure [11]. The other parameters included in the fit were the inhibition constant Ki' as no previous quantification of the parameter has been made, and r which is the reinvasion efficiency we are interested in. The identifiability of, and correlation between sets of parameters were checked by investigating the appearance of the minimum in the objective function used for fitting, as a function of two selected parameters. This was repeated for all 5 combinations of parameters (see Fig 4.10)

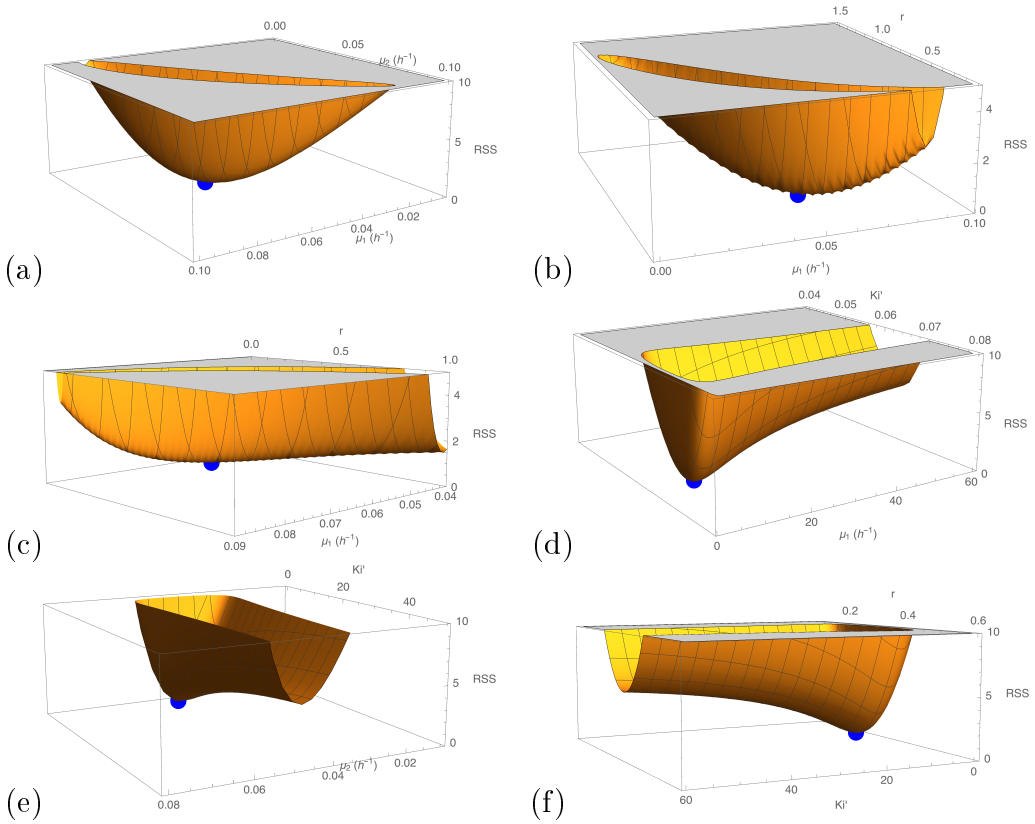

Figure 4.10: **Identifiability of the mechanistic model parameter combinations.** Identifiability of parameter combinations was tested by plotting RSS values for model fits on the z-axis over ranges of each parameter on the x-axis and y-axis respectively

In Fig.4.10 for each of the parameters of interest, a identifiability plot was constructed by plotting the changes of each pair with the goodness of fit or residual sum

of squared differences. What is also shown in these plots is the optimum values for the parameters obtained in the minimization procedure, by the re-parameterization of the model using experimental data. Fig.4.10(a) μ *vs* μ_2 (b) μ *vs* r show strong correlation between the parameter pairs evident from the furrow/groove, there is however a clear minimum and the optimum values for the parameters could be identified. The correlation between μ_2 *vs* r in Fig.4.10(c) seem to be the biggest challenge for accurate identification of the specific values. The total lactate is not very sensitive to the effect of Ki' which explains how the model can allow variance in this parameter and still obtain accurate results. Future studies must address more detailed studies on the inhibition and the identifiability will improve as the mechanism of the inhibition is better understood. The last three identifiability plots all include Ki' and similarities in Fig.4.10 (d,e,f) are evident. Although a minimum can be obtained, the increase in goodness of fit is not overwhelming. This is due to the fact that the apparent inhibition constant Ki' contributes minimal to the total lactate and big variance in this parameter does not lead to an significant decrease in goodness of fit. The model is therefore not very sensitive to Ki'.

The identifiability plots displayed that a minimum was obtained for each of the parameter combinations even though it was not always a well-defined minimum. The final set of parameters used in the fitting procedures is tabulated in Table 4.7.

Table 4.7: **Parameters for mechanistic model fits on experimental data** Each of the parameters with their respective units and the source of the quantities; experimentally determined (Exp) or obtained from parameter identification during the fit (Fit)

Pars	Description	Source	Units
$biomass$	Parasitic volume	Exp	fL/ml incubation
k_{Pf}	Parasitic lactate production	Lit*	$\frac{\mu moles\ Lac}{\mu L\ parasiticbiomass} \cdot h^{-1}$
Ki'	Apparent inhibition constant	Fit	mM
k_{uRBC}	uRBC lactate production	Exp	$\frac{\mu moles}{fL_{\text{RBC}}} \cdot h^{-1}$
par	The percentage of RBC infected with *P.falciparum*	Exp	%
r	reinvasion efficiency	Fit	Decimal fraction
RBCs	Number of RBCs in an incubation	Exp	-
μ	Specific growth rate of cycle 1	Fit	h^{-1}
μ_2	Specific growth rate of cycle 2	Fit	h^{-1}
tR	time of Reinvasion	Exp	$38 - 50h$

* (Du Toit, 2015)

Mechanistic model fit results As mentioned in Table 4.7, μ and μ_2 represent the specific growth rates of the 2 cycles. For the phenomenological model, we used independent specific growth rates as we wanted to approach the data based on minimal mechanistic knowledge. In the mechanistic model however, one would expect

that the specific growth rate should stay constant over both cycles if the external conditions do not change too much. We therefore start by A) constraining $\mu = \mu_2$ for the first data analysis, with the reinvasion efficiency constrained between the fractions 0.01 and 0.99. Although a constant specific growth rate is what we would expect over both cycles, the phenomenological model fit showed a decrease in the specific growth rate in the second cycle. To account for possible changes in the specific growth rate, we repeated the fit to include B) independent μ's (Table 4.9) and thereafter to also include C) the time of reinvasion as parameter (Table 4.10).

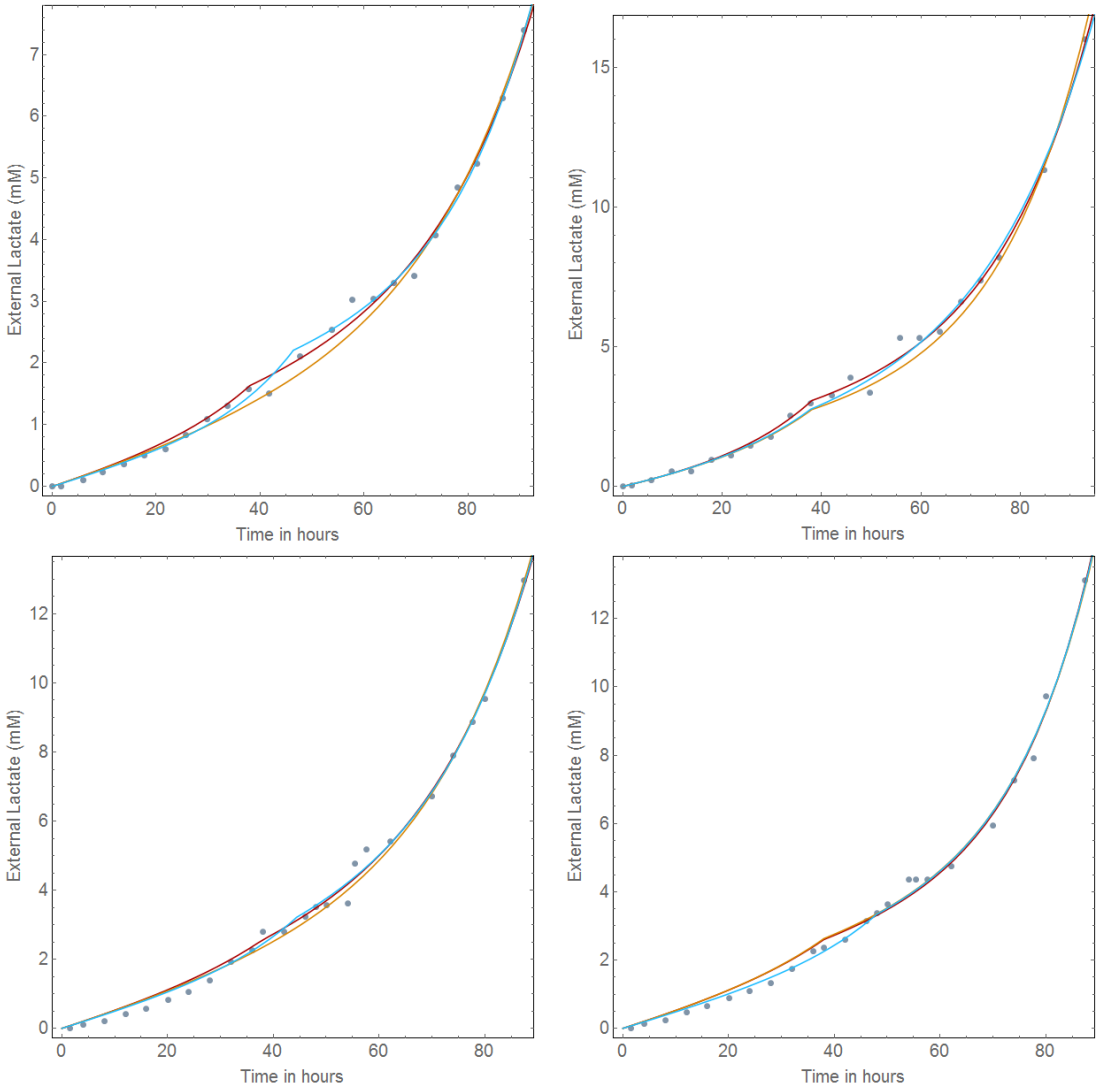

Figure 4.11: **Mechanistic model fits** The yellow simulation from $t = 0$ $(10hpmi)$ is of A) the first fit where μ stays constant, B) the dark red shows the independent μ for each cycle, but with a fixed reinvasion point of $t = 38h$ $(48hpmi)$ and C) the cyan simulation shows the independent μ and reinvasion time fits

Big differences in the accuracy of the three different analyses are not very obvious from the graphs. All three analysis methods seem to give a fairly accurate prediction of the lactate production. From Fig.4.11 analysis C, however, seemed to over predict

Table 4.8: A) Result of fit with constant μ over both cycles

	RSS	μ (h^{-1})	Ki'	r (decimal fraction)
Exp1	1.19	0.0455	7.34	0.92
Exp2	3.30	0.0561	15.89	0.32
Exp3	2.89	0.0498	12.06	0.99
Exp4	2.87	0.0643	7.51	0.34
Exp5	61.61	0.0902	25.24	0.02
Exp6	11.90	0.0596	*	0.44
Exp7	4.25	0.0211	*	0.99
Exp8	3.30	0.0832	*	0.10
Exp9	17.42	0.0369	*	0.99

*Experimental data for inhibition studies were not available to obtain optimum K_i values and the model was constrained to value range of first five experiments, the blue highlighted cells represent the experiments where the model could not find optimum fitted values for the parameters.

the time of reinvasion in Exp 1,2 and 4. All three of the analyses seems to overestimate the lactate production in Exp 3 and 4, which could be due to error in the biomass calculations which were one of the experimentally determined parameters. Further mathematical data analyses are needed to compare the different analyses more accurately. The detailed parameter identification results of each of the three analyses can be seen in Tables 4.8, 4.9, 4.10.

When constraining $\mu = \mu_2$ the model fails to identify optimum values for Exp 3,5,7 and 9. Reinvasion efficiencies of 0.92 and 0.1 for Exp 1 and Exp 8 are identified respectively which is biologically very unlikely.

By fitting for both μ and μ_2 independently, a great improvement is observed as the model only fails to find optimum values for Exp 7 and Exp 9.

Table 4.9: B)Result of fit with independent μ's for each cycle with a fixed reinvasion point (38h)

	RSS	$\mu_1(h^{-1})$	$\mu_2(h^{-1})$	Ki'	r (decimal fraction)
Exp1	0.75	0.0660	0.0489	7.43	0.345
Exp2	1.68	0.0633	0.0515	16.34	0.272
Exp3	2.50	0.0608	0.0498	11.86	0.627
Exp4	2.83	0.0631	0.0664	7.58	0.333
Exp5	14.81	0.0763	0.0368	16.42	0.338
Exp6	10.25	0.0686	0.0659	*	0.266
Exp7	1.05	0.0100	0.1447	*	0.111
Exp8	1.10	0.0801	0.0389	*	0.317
Exp9	2.50	0.0100	0.1267	*	0.415

*Experimental data for inhibition studies were not available to obtain optimum K_i values and the model was constrained to value range of first five experiments, the blue highlighted cells represent the experiments where the model could not find optimum fitted values for the parameters.

Table 4.10: C) Result of fit with independent μ's for each cycle and time of reinvasion point

	RSS	μ_1 (h^{-1})	μ_2 (h^{-1})	Ki'	r (decimal fraction)	$t_R(h)$
Exp1	0.66	0.0785	0.0595	7.38	0.217	46.4
Exp2	2.04	0.0565	0.0449	15.94	0.452	37.7
Exp3	2.40	0.0727	0.0526	11.91	0.500	44.4
Exp4	2.59	0.0723	0.0648	7.45	0.469	48.0
Exp5	14.80	0.0751	0.0364	*	0.350	37.0
Exp6	8.56	0.0867	0.0624	*	0.178	40.0
Exp7	1.04	0.0100	0.1308	*	0.130	36.3
Exp8	1.06	0.0807	0.0488	*	0.233	39.2
Exp9	0.51	0.0567	0.0719	*	0.350	35.9

*Experimental data for inhibition studies were not available to obtain optimum K_i values and the model was constrained to value range of first five experiments, the blue highlighted cells represent the experiments where the model could not find optimum fitted values for the parameters.

Akaike Information Criteria (AIC) When comparing a collection of models for a specific data set, the AIC values can be used as a tool to estimate the relative quality of the various models. When using finite sample sizes it is used with a statistical correction, AICc. As the AICc values do not include the use of a null hypothesis the purpose is not to obtain an ultimate measure of fitness but rather to compare models within a specific situation. The AICc values are calculated with Eq.4.2.17 and gives a measure of the benefit of an improved RSS vs the cost of a more complicated model (by the inclusion of an additional parameter), where a lower AICc value indicates an increased goodness of fit that was significant despite

Table 4.11: The AICc values for the mechanistic model fits

	A	B	C
Exp1	-50.50	**-55.48**	-54.98
Exp2	-26.17	**-33.25**	-27.64
Exp3	-38.98	**-39.04**	-37.09
Exp4	-37.49	**-35.26**	-34.09
Exp5	14.68	**-6.33**	-3.69
Exp6	**-0.11**	1.23	2.58
Exp7	-4.75	**-13.07**	-9.39
Exp8	-2.96	**-6.95**	-2.86
Exp9	3.86	**-13.48**	-26.88
AVE	-15.82	**-22.40**	-21.56
STDEV	± 21.80	± 21.06	± 20.04

the cost of an included parameter [88].

By including the independent μ_2 for the second cycle in analysis B (4.9) and t_R in analysis C (4.10), the fit is bound to improve, and therefore have a better RSS value. The necessity of the μ_2 values in the fitted parameters were subsequently tested by comparing of the AICc values of the three fits (A,B,C).

$$AICc = nLog(\frac{RSS}{n}) + 2K + \frac{2K(K+1)}{n-K-1}. \tag{4.2.17}$$

where n is the sample size, K is the number of parameters fitted and RSS the residual sum of squared differences

At first the mechanistic model was constrained to fit a constant specific growth rate over both cycles, based on the assumption that it should remain constant for a specific *P. falciparum* strain. It was difficult to obtain optimum fits for some of the experiments (Table 4.8). Thereafter independent growth rates were also fitted (analysis B, Table 4.9) and the reinvasion time (analysis C, Table 4.10). The AICc values were calculated for each of the experiment analysed with each analyses (A,B,C) and the results displayed in Table 4.11 with the lowest AICc values in bold. Although the averages of AICc values between specific analyses did not have significant differences, it was evident that analysis B returned the lowest AICc values for each of the experiments except Exp 6. We found that despite fitting for parameter μ_2 to the data (B), the quality of fit improved more than the cost of using an additional parameter. When the t_R is included in the fit (C), the quality of the fit did indeed improve, but the Akaike values increased. This leads to the conclusion that fit B, is the best to describe the data.

Merozoite Calculation In order to calculate the number of merozoites released per schizont, the fitted value for the reinvasion efficiency is used in combination with

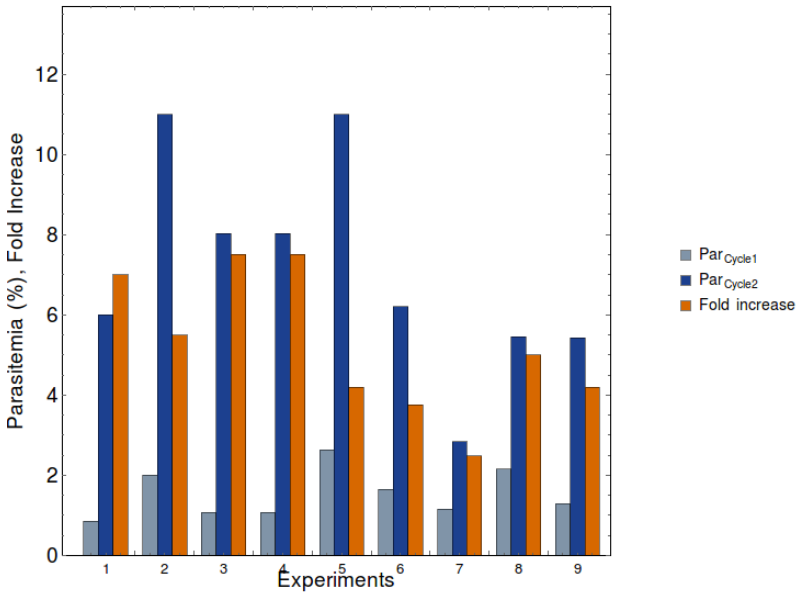

Figure 4.12: **Fold increase in parasitaemia.** During the experiments microscopy techniques are used to determine the parasitaemia during each cycle from which the fold increase was calculated for each experiment.

the parasitaemia, determined microscopically. In Fig. 4.12 the parasitaemia for each of the cycles in the individual experiments is shown. It appears that lower starting parasitaemia in Exp 1,3,4 lead to a higher fold increase, which was also observed by Reilly et al. [10]. Experiment 7 had the lowest fold increase in parasitaemia of only 2.48 and appears to be an outlier within the datasets.

We used the reinvasion efficiency results from the mechanistic model fits (Tables 4.8, 4.9 and 4.10) to estimate the number of merozoites with Eq. 4.1.19, as explained in the previous section (4.1.2.1), the parasitaemias measured in the experiments, and the results are shown in Table 4.12

According to analysis A) the reinvasion efficiency was 57.0%±40% and the number of merozoite released was 21.0±17.7. Analysis B) determined a reinvasion efficiency of 33.6%±13.7% and merozoites produced, 16.6±4.1. Using analysis C) the reinvasion efficiency and merozoite production was calculated as 32.0 ± 13.6 and 17.6 ± 7.1. In each of these analyses, the model could not be fitted to the data of Experiment 7 successfully which could be due ill growth, that resulted in the experiment to be an outlier. As each experiment was executed with changes in the experimental conditions, the reinvasion efficiency is not expected to stay exactly the same which explains he big standard deviations in these parameters. We do however expect that the average number of merozoites that are released per schizont to be constant for the *P.falciparum* strain if it is regulated by specific checkpoints during the life cycle under optimum conditions. Analysis B shows the lowest standard deviation for the merozoite production which also confirms the result of the Akaike values, that this analysis describes the data the best, resulting in a final average merozoites produced

Table 4.12: The average merozoites produced by schizonts in each experiment

			A		B		C	
	Par1	Par2	r	mer	r	mer	r	mer
Exp1	0.86%	6.00%	0.92	7.6	0.345	20.3	0.217	32.3
Exp2	2.00%	11.00%	0.32	16.0	0.272	18.7	0.452	11.3
Exp3	1.07%	8.03%	0.99	7.6	0.627	12.0	0.500	15.0
Exp4	1.07%	8.03%	0.34	22.1	0.333	22.6	0.469	16.0
Exp5	2.63%	11.00%	0.02	177.7	0.338	12.4	0.350	12.0
Exp6	1.65%	6.20%	0.44	8.4	0.266	14.1	0.178	21.1
Exp7	1.15%	2.84%	0.99	2.5	0.111	22.4	0.130	19.1
Exp8	2.15%	10.78%	0.10	50.9	0.317	15.8	0.233	21.5
Exp9	1.29%	5.43%	0.99	4.3	0.415	10.1	0.350	12.0
AVE			0.570	21.01	0.336	16.55	0.320	17.64
STDEV			0.40	17.72	0.137	4.07	0.136	7.12

where A) Constant μ's over both cycles, fixed reinvasion time, B) Independent μ's over both cycles, fixed reinvasion time, C) Independent μ's over both cycles, fit for reinvasion time

per schizont of 16 ± 4.

4.2.4 Comparison of phenomenological and mechanistic models

In this chapter two models were constructed to describe the reinvasion event between two intra-erythrocytic parasitic life cycles; a phenomenological model and a mechanistic model. The models were fitted to experimental metabolic data.

Modelling approach The first model was constructed with minimal biological information, and fitted on the experimental results, which we called the phenomenological model. Lactate production was measured, and from a mathematical view point, the data could be described well with exponential functions similarly to Du Toit [11]. Step by step the mathematical functions were applied to the experimental data to include new parameters (μ_2 *and* t_R) to improve the lactate predictions by the model around the reinvasion point.

Based on a theoretical derivation of lactate production by the parasite, the tangents of the lactate produced by the parasite at the reinvasion point could be used to calculate the reinvasion efficiency. This principle was used to calculate the reinvasion efficiency in four different exponential analyses. The basic exponential function was expanded to include biological influences on the lactate production and the reinvasion efficiency. This included the contribution of uRBCs to the total lactate and the inhibition of the uRBCs.

The advantage of this approach is that simple experiments can be used to study the reinvasion process with gradient ratios. The disadvantage of this model is that it disregards biological mechanisms. For our study on the reinvasion, we needed the pRBC lactate production and not the total lactate produced by both pRBCs and uRBCs. To account for this, we had to make corrections to the data. The simplicity of the model was therefore partly lost in the process.

To address the biological mechanisms better, a more mechanistic model was constructed. The approach to construct the mechanistic model was based on each of the contributors to the total lactate in a pRBC culture. From previous knowledge [11] we have independent mechanistic insight to how lactate is produced by the pRBC and the uRBCs. The iRBC could be described with a basic inhibitory mechanism using lactate produced by pRBCs as proxy. As the inhibition is still not fully elucidated the model still contains an aspect of a phenomenological character to include the inhibition of the uRBC in the model.

The two big differences between the two modelling approaches are the inclusion of uRBC inhibition and most importantly how the reinvasion efficiency is calculated or obtained. In the phenomenological model the inhibition of uRBCs is incorporated by correcting the data with a fixed inhibition. The mechanistic model however, include fits on experimental data for the iRBCs. Where in the phenomenological model the reinvasion efficiency is calculated from independently fitted exponential functions, the parameter is included into the mechanistic model and obtained during the fitting process.

Parameter identification As the phenomenological model describes the data with basic exponential functions, the parameters are not very well defined as various underlying biological mechanisms are combined in the parameters. For example in *analysis I,II* the parameters,a, a_2, represent the total lactate and we are thus unable to distinguish between lactate produced by the growing parasite or lactate initially present in the culture. The identification of the parameters in the phenomenological model does not hold much biological value.

The strength of the mechanistic model is the fact that the majority of the parameters are measured experimentally, to limit the fitted parameters. This means that all the parameters were well defined, except μ_2, and Ki' as this is linked to the inhibition of the uninfected RBC.

Comparison of fitted values of parameters to literature The parameters that describe the number of uRBCs and parasitaemia were determined microscopically and are dependent on the experimental set-up. The parasitaemia's obtained within the cultures were around 1-6%. The cell counts and parasitaemias where used to determine the biomass in fl using the volume of $10h$ *pmi* rings, $5fl$ [11].

The parameter describing the time of reinvasion also describes the duration of the life cycles. A life cycle is defined by the period between two successive RBC lysis events. This was determined experimentally and substituted into the model fittings. The time of reinvasion was only fitted in the third mechanistic model fit (C) and led to reinvasion times of between $35.9h$ and $48.0h$ experimentally, which is $45.9h$ and $59.0h$ *pmi* which is quite a big range. The literature value for the *P.falciparum* cycle time is $48h$ but differs between cultures and can vary due to various conditions [67]. Even though the number of merozoites are expected to stay constant under normal conditions, it is not yet known if the parasites compromise on cycle time, quantity of merozoites or volume of merozoites under stressed conditions. The other reason that could also lead to the result of a such a high value for the reinvasion time is that the experimental cultures do not have perfect synchronicity which could lead to difficulty in finding the optimal value in the model fits.

The specific growth rate is used to describe how fast cells/biomass in a culture divide based on the doubling rate. The phenomenological model resulted in $\mu_1 = 0.0656 \pm 0.012$ and $\mu_2 = 0.0329 \pm 0.005$ for *analysis I,II* , $\mu_1 = 0.0656 \pm 0.012$ and $\mu_2 = 0.0508 \pm 0.018$ for *analysis III* and $\mu_1 = 0.0421 \pm 0.016$ and $\mu_2 = 0.0498 \pm 0.018$ for *analysis IV*. It is interesting to notice that the specific growth rate decrease in the second cycle by $\pm 50\%$ in *analysis I,II* but when the model has the freedom to adjust for lactate present at the start of the second cycle in *analysis IV* the decrease in specific growth rate is only $\pm 22\%$. One would expect the specific growth rate to stay constant between the two cycles in the same experiment, but experimental conditions could have an influence.

The specific growth rate in *analysis IV* is less than in *Analysis I,II,III*, which could be due to an overcompensation in the parameters $c1, c2$, which were included to describe external lactate at $t = 0h$ and $t = 38h$. The mechanistic model fit resulted

in $\mu = 0.0692 \pm 0.008\, h^{-1}$ for the constant μ fits and $\mu_1 = 0.0733 \pm 0.006\, h^{-1}$ and $\mu_2 = 0.0590 \pm 0.013\, h^{-1}$ for the independent μ fits. These results compare very well to findings by Du Toit [11] and Saliba [89].

Du Toit [11] showed that the specific growth rate of the parasite volume was $\mu = 0.0719\, h^{-1}$. It can also be calculated from the amount of growth in volume over a specific time. The parasite volume increase in Du Toit's [11] and Saliba's [89] work can be used to calculate specific growth rates, resulting in $0.0595 - 0.0665\, h^{-1}$.

The apparent inhibition constant (Ki') that was fitted in the mechanistic model does not hold biologically significant value as it is a ratio between two inhibition constants. Currently, there exist no knowledge about the nature of this inhibition constant.

As the mechanistic model described the data better and analysis B was the best of the three mechanistic analysis procedures we decided to use the results of analysis B as it had the best fit and the lowest AICc value, and lowest variance in number of merozoites produced. The final reinvasion efficiency was determined as $33.6\% \pm 13.7\%$. It is an average between 9 different experiments so we expect some variation in efficiencies, but it reveals that the reinvasion efficiency found in our study is comparable to Reilly et al. [10] and Kerlin et al. [67]. It was previously suggested that the reinvasion efficiency is between 25% by Reilly et al. [10] and 30% by Kerlin et al. [67] but as it is so difficult to study the reinvasion, previous studies rather focused on the increase in parasitaemia.

The number of merozoites is very similar to what is shown in previous literature which range from 8 to 30 as described by Cowman et al.[46], Harvey et al. [47] and Kerlin et al. [67]. We could decrease the range to between 12.4 and 20.3 with an average of 16 ± 4 determined with the mechanistic model fit B.

Culturing malaria parasites still remains challenging which makes it very difficult to repeat an experiment with the exact culture conditions. The parasites are sensitive to the RBCs they are cultured in and the synchronising method. This is very important as the synchronicity of the culture has a big influence on the identification of the parameter t_R which in turn has an influence on the specific growth rate and the reinvasion efficiency.

Comparison to methods used in literature As mentioned in Chapter 2, current methods mostly depend on microscopical techniques where a limited number of cells are studied. By studying whole cultures, our sample sizes are much bigger which gives more reliable data as the outcome doesn't depend on just a few hundred cells.

Using the lactate production of the cultures is a completely new method to study reinvasion and can be used to gain insight on the biological mechanisms on a different level then previously done. This method is not limited to the outcome of the number of merozoites produced, but is the start of understanding the reinvasion

mechanisms quantitatively and construction of a mathematical model for the process. The methods and model constructed in this thesis can be used to further study reinvasion efficiency under various other conditions to broaden our understanding of the reinvasion and how it is influenced by different stress-situations. There is a special interest in the few minutes that merozoites invade new RBCs and a better understanding of the molecular aspects of invasion will pave the way for development of novel targets and prophylactic solutions to malaria [10, 47].

Potential of whole body modeling The knowledge gained can be included in other models that describe the life cycle of the parasites. One of these models that could benefit from this is the combined metabolic model of Penkler [16] and Mulquiney [17] by Du Toit [11]. This model has been used to identify possible drug targets within the metabolic pathway and will be able to predict the outcome of targeting various enzymes therapeutically, as the model becomes more accurate and is scaled up to whole body models. Snoep et. al. [90] explores the potential of these incorporated models to predict the effect of drug-inhibition on reaction steps on the whole-body physiology.

Chapter 5

Concluding Remarks

In malaria patients, clinical symptoms that emerge are anaemia, lactic acidosis, fever, hypoglycaemia and neurological pathologies [2, 8]. A major cause of morbidity and possible mortality is anaemia [2]. The ability of the parasite to achieve high parasite densities facilitates the degree of clinical symptoms of malaria.The invasion is an important step for the replication and survival of the parasites, and we still have limited knowledge on the process.

Aims and Objectives The aim of this project was to quantify the reinvasion event mathematically, in terms of the reinvasion efficiency and the average number of merozoites produced per schizont, using experimental observations of metabolism of parasites and RBCs. The research questions that emerged were: i) Is it possible to use simple exponential equations as a phenomenological model to describe the lactate production over parasitic life cycles to study the reinvasion efficiency? ii) What is the contribution of uRBC lactate production in the system and how is it influenced in the presence of growing parasites? iii) Can we construct a mechanistic model that describes the lactate production of a parasitized RBC culture based on the changes in biomass that occur during the reinvasion process?

To address these questions the following objectives were achieved: A phenomenological model was constructed that consisted of two exponential functions for the two growth cycles. A growth cycle is defined as the period between successive cell divisions wherein a parasite grows from a merozoite to a schizont which bursts to release daughter merozoites. An important attraction of the phenomenological model is that it is completely unbiased, consisting of two independent exponential equations fitted to the data.

We found that the phenomenological model fitted the data well, but when these fits where interpreted mathematically to gain the reinvasion efficiency we found big variance in both the reinvasion efficiency and the number of merozoites. This is due to the over simplification of more complex biological mechanisms.

As we learnt more about the system and included various parameters for external lactate and the lactate contribution of the uRBCs, the model moved away from a

completely unbiased one. The phenomenological model was a first step to describing the reinvasion event quantitatively and we used the insights gained in the process for the construction of our mechanistic model.

The second objective, to quantify the observed inhibition by the parasites on the uRBCs glycolytic activity, was achieved in Section 4.2.2 by using lactate as a proxy for the hypothetical inhibitor of the uRBC in the presence of pRBCs. This was supported by the findings that pH and external lactate could not be accounted for the inhibition on the uRBCs, and that the inhibition over time showed a similar trend to the exponential increase in biomass over time measured as lactate.

The mechanistic model was constructed by describing the change in biomass, lactate production by pRBCs, lactate production by uRBCs and the inhibitory effect experienced by the uRBCs mathematically in Section 4.2.2 and thereby achieving the third objective.

For the fourth objective, the model was tested by simulating it with experimentally determined parameters, and including literature values for specific growth rate μ, reinvasion efficiency r and the apparent inhibition constant K_i. The test fits using the literature values showed that the model can describe the experimental data well. Subsequently the model was fitted to the experimental data to obtain fitted values for specific growth rate μ, reinvasion efficiency r and the apparent inhibition constant K_i. The identifiability of these were confirmed using identifiability plots. The tested model described the data reasonably accurate and we proceeded to fit the model to experimental metabolic data to obtain new values for the μ, r, K_i and t_R and thus succeeding in our fifth objective.

Finally for the sixth objective the reinvasion efficiency and the number of merozoites released per schizont were determined as $33.6\% \pm 13.7\%$ and 16 ± 4 respectively and these values are comparable to what has been documented in literature. This indicates that the mechanistic model is a good tool to study the reinvasion further.

Improvements and Future Studies The reinvasion is dependent on various factors that have been studied independently, also explained in Chapter 2. These include: receptor-ligand interactions, merozoite half-life, the motile response, metabolic triggers and the susceptibility of RBCs (dynamics within the blood stream, the age class and RBC pathologies). In terms of experimental set-up we have kept the experimental conditions as constant as possible and therefore expect that the reinvasion efficiency would vary slightly but we expect the average number of merozoites to vary minimally. The current model simulation can be improved by including more experimental data for the fit. This is very important for the inhibition of uRBC and the next step could include doing more enzyme specific experiments using the spent culture media to gain insight into the mechanism of the inhibition and to try and identify the inhibitor.

The time of reinvasion has a big effect on the model fitting and as culturing malaria is a challenge, obtaining a perfectly synced culture as assumed by the model is

unachievable. Our synchronisation methods can be improved to get a shorter window in which reinvasion occurs, which will result in experimental data with higher quality and better fits. The other option is to improve the model by including a degree of asynchronicity, this will also allow the model to be more accurate when applied to data from patients.

In future we can fit our model to experimental data of different parasitaemias and different percentages of hematocrit to study how the reinvasion is influenced in terms of reinvasion efficiency, number of merozoites released and changes in specific growth rates. The inhibition of the uRBC could be studied further to obtain more insight on the specific mechanism. This could be done by using the spent media of pRBCs on specific enzymes like PFK and PK.

Future work also includes expanding the model to whole-body description of glucose metabolism which will allow us to gain insight into the pathological symptoms such as lactic acidosis and hypoglycaemia experienced by patients infected with *P. falciparum* and disruption of glucose homeostasis during the intra-erythrocytic phase of the parasite's life cycle.

Finally, the current model is based on synchronised malaria cultures, which differs greatly if compared to the dynamics within a human host blood circulatory system as new factors come in play eg. higher haematocrit, lower parasitaemias, more turbulent forces, changes in nutrient availability, metabolism and removal of lactate and the cause of inhibition on the uRBCs. The model can be be fitted to longitudinal data of parasitaemia in malaria patients to get an estimate on reinvasion efficiency in patients and to bridge the gap between the knowledge based on cultures to cases of malaria infection in humans.

Conclusions To conclude, we found that it was possible to describe the reinvasion event with simple phenomenological equations, but more accurate results were obtained when additional factors for biological processes that influence the total lactate production were included. The inhibition experienced by uRBCs revealed strong correlation to the pRBCs lactate production and was therefore described mathematically by using the pRBC lactate production as a proxy. A mechanistic model was created that could predict the lactate production over two intraerythrocytic *P. falciparum* cycles including the reinvasion event. The model was fitted to experimental metabolic data and parameter values from the fits were used to calculate an average reinvasion efficiency of $33.6\% \pm 13.7\%$, the average merozoites released could subsequently be calculated and resulted in an average of 16 ± 4.

Chapter 6

Appendix

6.1 Phenomenological fits

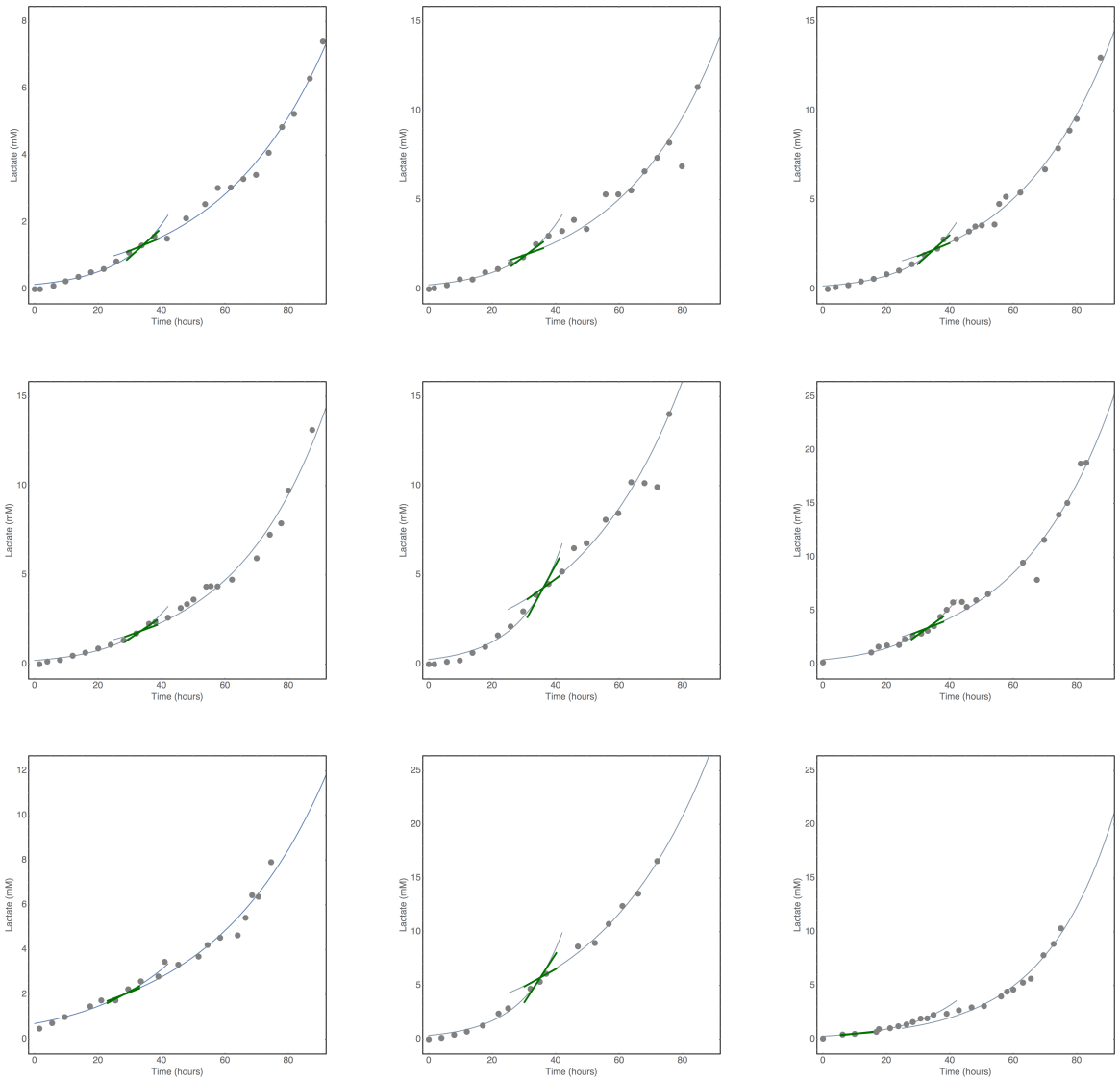

Figure 6.1: **A phenomenological model(I)** Experimentally determined lactate production of synchronised *P. falciparum* cultures fitted with simple exponential equations 4.1.1, 4.1.2 (grey line). The rate of lactate production just before and after reinvasion is shown in green.

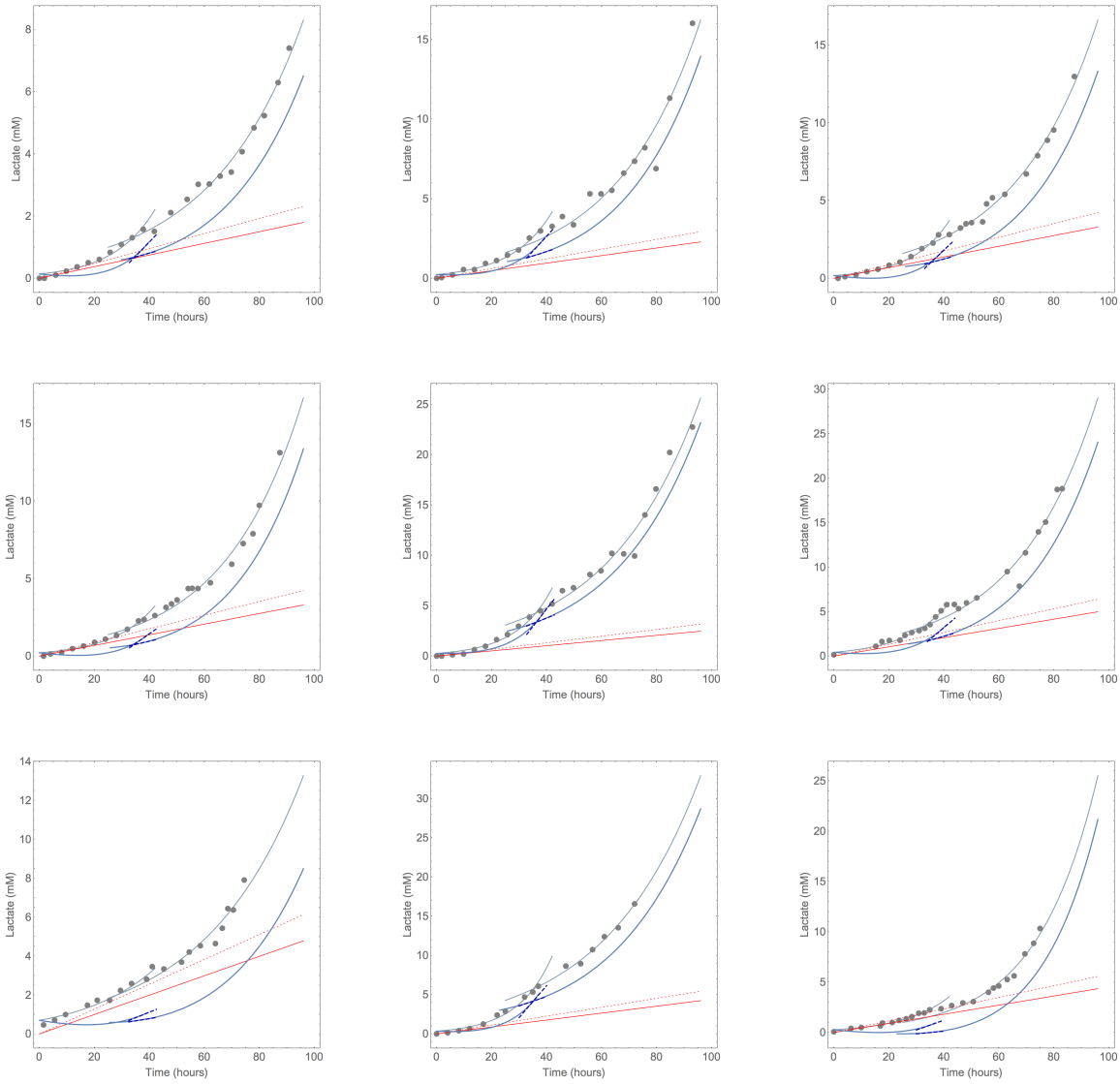

Figure 6.2: **Phenomenological model(II) fits to *P. falciparum* lactate production over two life cycles.** The solid blue lines represent the corrected lactate production for pRBCs. The two tangents at the point of reinvasion shows the rate of lactate production by pRBCs at the end of the first cycle and the start of the second cycle.

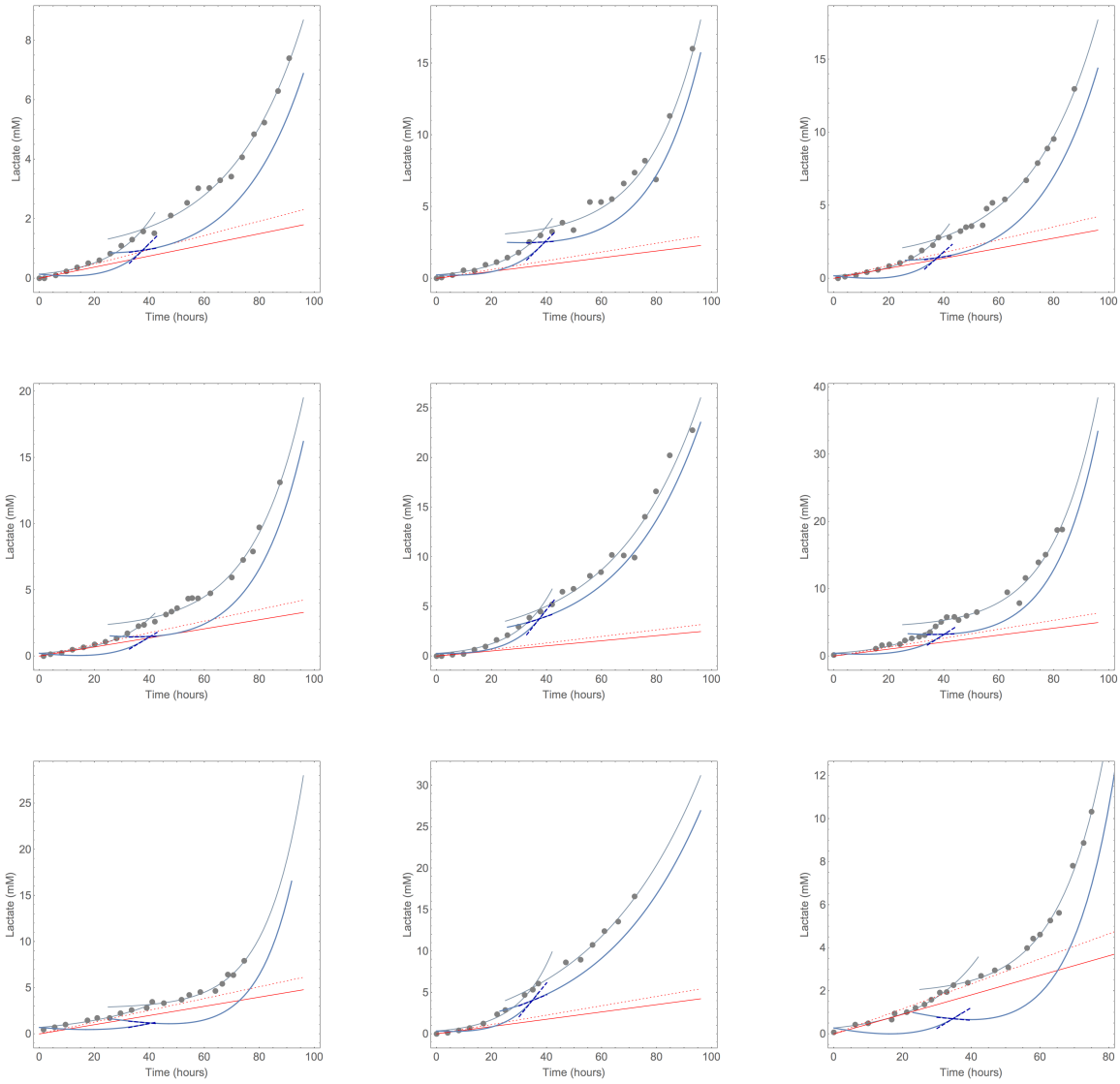

Figure 6.3: **The lactate production in pRBCs fitted with the adjusted phenomenological model(III)** fits Eq.4.1.14,4.1.15. Lactate production of uninhibited uRBCs are shown with the dotted red line and the solid red line represents the lactate contributed to the incubation by iRBCs. The solid blue lines represent the corrected lactate production for pRBCs. The two darker blue tangents at the point of reinvasion shows the rate of lactate production at the end of the first cycle and the start of the second cycle.

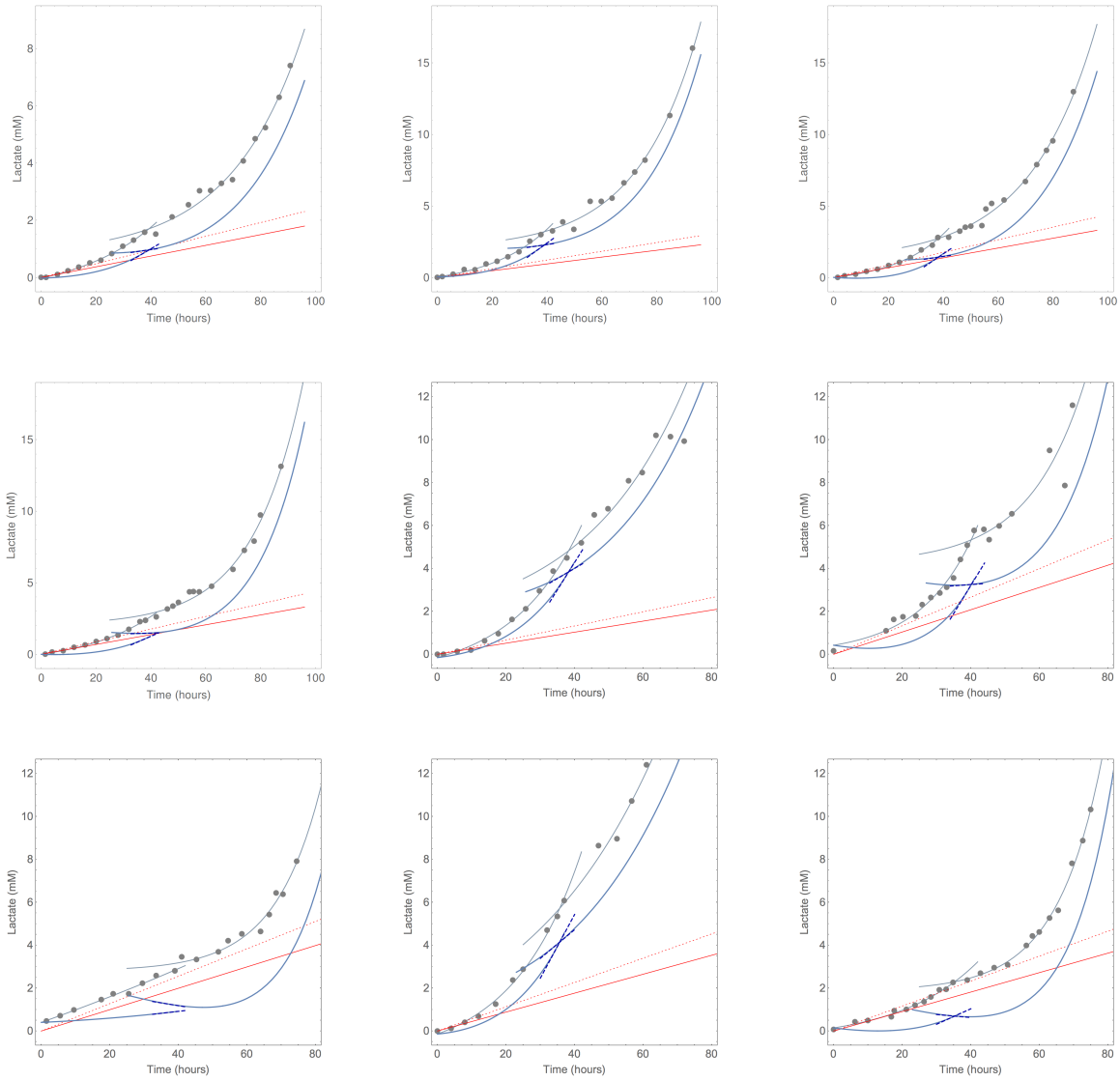

Figure 6.4: **The lactate production in pRBCs fitted with the adjusted phenomenological model(IV)** fits Eq.4.1.16. Lactate production of uninhibited uRBCs are shown with the dotted red line and the solid red line represents the lactate contributed to the incubation by iRBCs. The solid blue lines represent the corrected lactate production for pRBCs. The two darker blue tangents at the point of reinvasion shows the rate of lactate production at the end of the first cycle and the start of the second cycle.

6.2 Mechanistic model fits

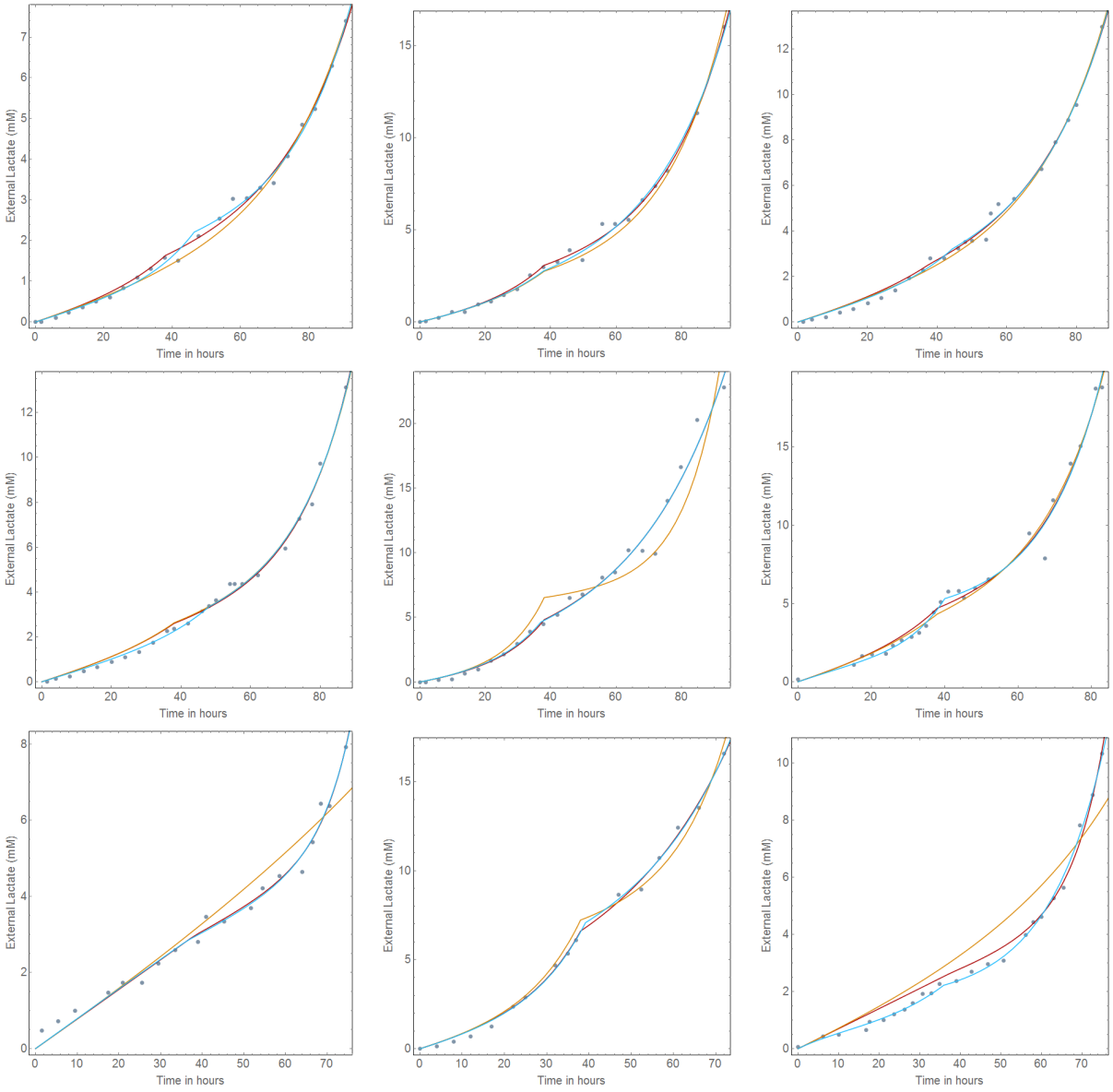

Figure 6.5: **Mechanistic model fits** The yellow simulation is of A) the first fit where μ stays constant, B) the dark red shows the independent μ for each cycle, but with a fixed reinvasion point and C) the cyan simulation shows the independent μ and reinvasion time fits

Bibliography

[1] Organization WH. World malaria report 2014; 2014.

[2] White NJ, Pukrittayakamee S, Hien TT, Faiz MA, Mokuolu OA, Dondorp AM. Malaria. Lancet. 2014;383(9918):723–735.

[3] Luxemburger C, Thwai KL, White NJ, Webster HK, Kyle DE, Maelankirri L, et al. The epidemiology of malaria in a Karen population on the western border of Thailand. Trans R Soc Trop Med Hyg. 1996;90(2):105–111.

[4] Moran JS, Bernard KW. The spread of chloroquine-resistant malaria in Africa. Implications for travelers. JAMA. 1989;262(2):245–248.

[5] Preuss J, Maloney P, Peddibhotla S, Hedrick MP, Hershberger P, Gosalia P, et al. Discovery of a Plasmodium falciparum Glucose-6-phosphate Dehydrogenase 6-phosphogluconolactonase Inhibitor (R, Z)-N-((1-Ethylpyrrolidin-2-yl) methyl)-2-(2-fluorobenzylidene)-3-oxo-3, 4-dihydro-2 H-benzo [b][1, 4] thiazine-6-carboxamide (ML276) That Reduces Parasite Growth in Vitro. Journal of medicinal chemistry. 2012;55(16):7262–7272.

[6] Dondorp AM, Nosten F, Yi P, Das D, Phyo AP, Tarning J, et al. Artemisinin resistance in Plasmodium falciparum malaria. New England Journal of Medicine. 2009;361(5):455–467.

[7] Boyle MJ, Wilson DW, Beeson JG. New approaches to studying Plasmodium falciparum merozoite invasion and insights into invasion biology. International Journal for Parasitology. 2013;43(1):1–10.

[8] Gerald N, Mahajan B, Kumar S. Mitosis in the human malaria parasite plasmodium falciparum. Eukaryotic Cell. 2011;10(4):474.

[9] Arnot DE, Ronander E, Bengtsson DC. The progression of the intra-erythrocytic cell cycle of Plasmodium falciparum and the role of the centriolar plaques in asynchronous mitotic division during schizogony. International Journal for Parasitology. 2011;41(1):71–80.

[10] Reilly HB, Wang H, Steuter Ja, Marx AM, Ferdig MT. Quantitative dissection of clone-specific growth rates in cultured malaria parasites. International Journal for Parasitology. 2007;37(14):1599–1607.

[11] Toit FD. Modeling glycolysis in Plasmodium-infected erythrocytes [Phd Thesis]. University of Stellenbosch. Stellenbosch, South Africa; 2015.

[12] Clark IA, Budd AC, Alleva LM, Cowden WB. Human malarial disease: a consequence of inflammatory cytokine release. Malaria Journal. 2006;5(1):1.

[13] Yau HK, Stacpoole PW. The Pathophysiology of Hypoglycemia and Lactic Acidosis in Malaria. 2014;.

[14] Mehta M, Sonawat HM, Sharma S. Malaria parasite-infected erythrocytes inhibit glucose utilization in uninfected red cells. FEBS letters. 2005;579(27):6151–6158.

[15] Mehta M, Sonawat HM, Sharma S. Glycolysis in Plasmodium falciparum results in modulation of host enzyme activities. Journal of vector borne diseases. 2006;43(3):95.

[16] Penkler GP. A Kinetic Model of Glucose Catabolism in Plasmodium falciparum. University of Stellenbosch; 2011.

[17] Mulquiney PJ, Kuchel PW. Model of 2, 3-bisphosphoglycerate metabolism in the human erythrocyte based on detailed enzyme kinetic equations1: equations and parameter refinement. Biochemical Journal. 1999;342(3):581–596.

[18] Biamonte MA, Wanner J, Le Roch KG. Recent advances in malaria drug discovery. Bioorg Med Chem Lett. 2013;23(10):2829–2843.

[19] Roberts J J Janovy. Foundations of Parasitology. McGraw-Hill:Dubuque; 2000.

[20] McAlister RO. Time-dependent loss of invasive ability of Plasmodium berghei merozoites in vitro. The Journal of parasitology. 1977; p. 455–463.

[21] Kirk K, Lehane AM. Membrane transport in the malaria parasite and its host erythrocyte. Biochem J. 2014;457(1):1–18.

[22] Lang-Unnasch N, Murphy A. Metabolic changes of the malaria parasite during the transition from the human to the mosquito host. Annual Reviews in Microbiology. 1998;52(1):561–590.

[23] Langreth SG, Jensen JB, Reese RT, Trager W. Fine structure of human malaria in vitro. The Journal of protozoology. 1978;25(4):443–452.

[24] Slomianny C. Three-dimensional reconstruction of the feeding process of the malaria parasite. Blood cells. 1989;16(2-3):369–378.

[25] Lew VL. Malaria: endless fascination with merozoite release. Current biology. 2005;15(18):R760–R761.

[26] Ferrer J, Vidal J, Prats C, Valls J, Herreros E, Lopez D, et al. Individual-based model and simulation of Plasmodium falciparum infected erythrocyte in vitro cultures. Journal of Theoretical Biology. 2007;248(3):448 – 459.

[27] Lew VL. Packaged merozoite release without immediate host cell lysis. TRENDS in Parasitology. 2001;17(9):401–403.

[28] Wickham ME, Culvenor JG, Cowman AF. Selective inhibition of a two-step egress of malaria parasites from the host erythrocyte. Journal of Biological Chemistry. 2003;278(39):37658–37663.

[29] Arnot D. Cell Cycle Regulation in Plasmodium. 2014;(January 2014):1–8.

[30] Mahajan B, Selvapandiyan A, Gerald NJ, Majam V, Zheng H, Wickramarachchi T, et al. Centrins, cell cycle regulation proteins in human malaria parasite Plasmodium falciparum. Journal of Biological Chemistry. 2008;283(46):31871–31883.

[31] Bannister L, Hopkins J, Fowler R, Krishna S, Mitchell G. A brief illustrated guide to the ultrastructure of Plasmodium falciparum asexual blood stages. Parasitology Today. 2000;16(10):427–433.

[32] Schrevel J, Asfaux-Foucher G, Hopkins J, Robert V, Bourgouin C, Prensier G, et al. Vesicle trafficking during sporozoite development in Plasmodium berghei: ultrastructural evidence for a novel trafficking mechanism. Parasitology. 2008;135(01):1–12.

[33] Aikawa M, Beaudoin RL. Studies on nuclear division of a malarial parasite under pyrimethamine treatment. The Journal of cell biology. 1968;39(3):749.

[34] Carvalho TG, Doerig C, Reininger L. Nima-and Aurora-related kinases of malaria parasites. Biochimica et Biophysica Acta (BBA)-Proteins and Proteomics. 2013;1834(7):1336–1345.

[35] Arnot D, Gull K. The Plasmodium cell cycle: facts and questions. Annals of tropical medicine and parasitology. 1998;92(4):361–365.

[36] Striepen B, Jordan CN, Reiff S, Van Dooren GG. Building the perfect parasite: cell division in apicomplexa. PLoS Pathog. 2007;3(6):e78.

[37] Hunt T. Nobel lecture: protein synthesis, proteolysis, and cell cycle transitions. Bioscience reports. 2002;22(5-6):465–486.

[38] Aikawa M, Huff CG, Sprinz H. Fine structure of the asexual stages of Plasmodium elongatum. The Journal of cell biology. 1967;34(1):229–249.

[39] Doerig C, Baker D, Billker O, Blackman M, Chitnis C, Dhar Kumar S, et al. Signalling in malaria parasites. The MALSIG consortium. 2009;.

[40] Doerig C, Endicott J, Chakrabarti D. Cyclin-dependent kinase homologues of Plasmodium falciparum. International journal for parasitology. 2002;32(13):1575–1585.

[41] Halbert J, Ayong L, Equinet L, Le Roch K, Hardy M, Goldring D, et al. A Plasmodium falciparum transcriptional cyclin-dependent kinase-related kinase with a crucial role in parasite proliferation associates with histone deacetylase activity. Eukaryotic cell. 2010;9(6):952–959.

[42] Kozlov S, C Waters N, Chavchich M. Leveraging cell cycle analysis in anticancer drug discovery to identify novel plasmodial drug targets. Infectious Disorders-Drug Targets (Formerly Current Drug Targets-Infectious Disorders). 2010;10(3):165–190.

[43] Reininger L, Tewari R, Fennell C, Holland Z, Goldring D, Ranford-Cartwright L, et al. An essential role for the Plasmodium Nek-2 Nima-related protein kinase in the sexual development of malaria parasites. Journal of Biological Chemistry. 2009;284(31):20858–20868.

[44] Reininger L, Billker O, Tewari R, Mukhopadhyay A, Fennell C, Dorin-Semblat D, et al. A NIMA-related protein kinase is essential for completion of the sexual cycle of malaria parasites. Journal of Biological Chemistry. 2005;280(36):31957–31964.

[45] Tewari R, Straschil U, Bateman A, Böhme U, Cherevach I, Gong P, et al. The systematic functional analysis of Plasmodium protein kinases identifies essential regulators of mosquito transmission. Cell host & microbe. 2010;8(4):377–387.

[46] Cowman AF, Crabb BS. Invasion of red blood cells by malaria parasites. Cell. 2006;124(4):755–766.

[47] Harvey KL, Gilson PR, Crabb BS. A model for the progression of receptor-ligand interactions during erythrocyte invasion by Plasmodium falciparum. International Journal for Parasitology. 2012;42(6):567–73.

[48] Cohen S, McGregor I, Carrington S, et al. Gamma-globulin and acquired immunity to human malaria. Nature. 1961;192:733–7.

[49] Boyle MJ, Wilson DW, Richards JS, Riglar DT, Tetteh KK, Conway DJ, et al. Isolation of viable Plasmodium falciparum merozoites to define erythrocyte invasion events and advance vaccine and drug development. Proceedings of the National Academy of Sciences. 2010;107(32):14378–14383.

[50] Hill DL, Eriksson EM, Schofield L. High yield purification of Plasmodium falciparum merozoites for use in opsonizing antibody assays. Journal of visualized experiments: JoVE. 2014;(89).

[51] Beeson JG, Crabb BS. Towards a vaccine against Plasmodium vivax malaria. PLoS Med. 2007;4(12):e350.

[52] Dvorak JA, Miller LH, Whitehouse WC, Shiroishi T. Invasion of erythrocytes by malaria merozoites. Science. 1975;187(4178):748–750.

[53] Gilson PR, Crabb BS. Morphology and kinetics of the three distinct phases of red blood cell invasion by Plasmodium falciparum merozoites. International journal for parasitology. 2009;39(1):91–96.

[54] Lew VL, Tiffert T. Is invasion efficiency in malaria controlled by pre-invasion events? Trends in parasitology. 2007;23(10):481–484.

[55] Bannister L, Dluzewski A. The ultrastructure of red cell invasion in malaria infections: a review. Blood cells. 1989;16(2-3):257–92.

[56] Glushakova S, Yin D, Li T, Zimmerberg J. Membrane transformation during malaria parasite release from human red blood cells. Current biology. 2005;15(18):1645–1650.

[57] Dluzewski A, Rangachari K, Gratzer W, Wilson R. Inhibition of malarial invasion of red cells by chemical and immunochemical linking of spectrin molecules. British journal of haematology. 1983;55(4):629–637.

[58] Dluzewski AR, Nash GB, Wilson RJ, Reardon DM, Gratzer WB. Invasion of hereditary ovalocytes by Plasmodium falciparum in vitro and its relation to intracellular ATP concentration. Molecular and biochemical parasitology. 1992;55(1):1–7.

[59] Dennis E, Mitchell G, Butcher G, Cohen S. In vitro isolation of Plasmodium knowlesi merozoites using polycarbonate sieves. Parasitology. 1975;71(03):475–481.

[60] Johnson J, Epstein N, Shiroishi T, Miller L. Factors affecting the ability of isolated Plasmodium knowlesi merozoites to attach to and invade erythrocytes. Parasitology. 1980;80(03):539–550.

[61] Salcedo-Sora JE, Caamano-Gutierrez E, Ward SA, Biagini GA. The proliferating cell hypothesis : a metabolic framework for Plasmodium growth and development. Trends in Parasitology. 2014;30(4):170–175.

[62] Mitchell GH, H BL. Malaria Parasite Invasion: Interactions with the red cell membrane; 1988.

[63] Iyer J, Grüner AC, Rénia L, Snounou G, Preiser PR. Invasion of host cells by malaria parasites: a tale of two protein families. Molecular microbiology. 2007;65(2):231–249.

[64] Haydon DT, Matthews L, Timms R, Colegrave N. Topndash; down or bottom–up regulation of intra–host blood–stage malaria: do malaria parasites most resemble the dynamics of prey or predator? Proceedings of the Royal Society of London: Biological Sciences. 2003;270(1512):289–298.

[65] Cromer D, Stark J, Davenport MP. Low red cell production may protect against severe anemia during a malaria infectionâĂŤinsights from modeling. Journal of theoretical biology. 2009;257(4):533–542.

[66] Pasvol G, Weatherall D, Wilson R. The increased susceptibility of young red cells to invasion by the malarial parasite Plasmodium falciparum. British journal of haematology. 1980;45(2):285–295.

[67] Kerlin DH, Gatton ML, Mons B, Antia R, Yates A, de Roode J, et al. Preferential Invasion by Plasmodium Merozoites and the Self-Regulation of Parasite Burden. PLoS ONE. 2013;8(2):e57434.

[68] Barnwell JW. Cytoadherence and sequestration in falciparum malaria. Experimental parasitology. 1989;69(4):407–412.

[69] Friedman MJ. Erythrocytic mechanism of sickle cell resistance to malaria. Proceedings of the National Academy of Sciences. 1978;75(4):1994–1997.

[70] Nagel RL, Raventos-suarez C, Fabry ME, Tanowitz H. Impairment of the Growth of Plasmodium Falciparum in HbEE Erythrocytes. Journal of Clinival Investment. 1981;68(July):303–305.

[71] Bannister L, Mitchell G. The ins, outs and roundabouts of malaria. Trends in parasitology. 2003;19(5):209–213.

[72] Prensier G, Slomianny C. The karyotype of Plasmodium falciparum determined by ultrastructural serial sectioning and 3D reconstruction. The Journal of parasitology. 1986; p. 731–736.

[73] Margos G, Bannister L, Dluzewski A, Hopkins J, Williams I, Mitchell G. Correlation of structural development and differential expression of invasion-related molecules in schizonts of Plasmodium falciparum. Parasitology. 2004;129(03):273–287.

[74] Fennell B, Al-Shatr Z, Bell A. Isotype expression, post-translational modification and stage-dependent production of tubulins in erythrocytic Plasmodium falciparum. International journal for parasitology. 2008;38(5):527–539.

[75] Tilley L, McFadden G, Cowman A, Klonis N. Illuminating Plasmodium falciparum-infected red blood cells. Trends in parasitology. 2007;23(6):268–277.

[76] Reininger L, Wilkes JM, Bourgade H, Miranda-Saavedra D, Doerig C. An essential Aurora-related kinase transiently associates with spindle pole bodies during Plasmodium falciparum erythrocytic schizogony. Molecular microbiology. 2011;79(1):205–221.

[77] Brown WM, Yowell CA, Hoard A, Vander Jagt TA, Hunsaker LA, Deck LM, et al. Comparative structural analysis and kinetic properties of lactate dehydrogenases from the four species of human malarial parasites. Biochemistry. 2004;43(20):6219–6229.

[78] Dunn CR, Banfield MJ, Barker JJ, Higham CW, Moreton KM, Turgut-Balik D, et al. The structure of lactate dehydrogenase from Plasmodium falciparum reveals a new target for anti-malarial design. Nature Structural & Molecular Biology. 1996;3(11):912–915.

[79] Roth EJ, Calvin MC, Max-Audit I, Rosa J, Rosa R. The enzymes of the glycolytic pathway in erythrocytes infected with Plasmodium falciparum malaria parasites. Blood. 1988;72(6):1922–1925.

[80] Visser D, Heijnen JJ. Dynamic simulation and metabolic re-design of a branched pathway using linlog kinetics. Metabolic engineering. 2003;5(3):164–176.

[81] Olszewski KL, Llinás M. Central carbon metabolism of Plasmodium parasites. Molecular and biochemical parasitology. 2011;175(2):95–103.

[82] Young HL, Pace N. Some physical and chemical properties of crystalline α-glycerophosphate dehydrogenase. Archives of biochemistry and biophysics. 1958;75(1):125–141.

[83] Kirk K. Membrane transport in the malaria-infected erythrocyte. Physiological Reviews. 2001;81(2):495–537.

[84] Jensen MD, Conley M, Helstowski LD. Culture of Plasmodium falciparum: the role of pH, glucose, and lactate. The Journal of parasitology. 1983; p. 1060–1067.

[85] Boogerd F, Bruggeman FJ, Hofmeyr JHS, Westerhoff HV. Systems biology: philosophical foundations. Elsevier; 2007.

[86] Trager W, Jensen JB. Human malaria parasites in continuous culture. Science. 1976;193(4254):673–675.

[87] Lambros C, Vanderberg JP. Synchronization of Plasmodium falciparum erythrocytic stages in culture. The Journal of parasitology. 1979; p. 418–420.

[88] Akaike H. Akaikes Information Criterion. In: International Encyclopedia of Statistical Science. Springer; 2011. p. 25–25.

[89] Saliba KJ, Horner HA, Kirk K. Transport and Metabolism of the Essential Vitamin Pantothenic Acid in Human Erythrocytes Infected with the Malaria Parasite Plasmodium falciparum. Journal of Biological Chemistry. 1998;273(17):10190–10195.

[90] Snoep JL, Green K, Eicher J, Palm DC, Penkler G, du Toit F, et al. Quantitative analysis of drug effects at the whole-body level: a case study for glucose metabolism in malaria patients. Biochemical Society Transactions. 2015;43(6):1157–1163.